Flexibility and hydration of amphiphilic hyperbranched arabinogalactan-protein from plant exudate: a volumetric perspective

Véronica Mejia Tamayo, Michael Nigen, Rafael Apolinar Valiente, Thierry Doco, Pascale Williams, Denis Renard, Christian Sanchez

HAL Id: hal-02154396

https://hal.science/hal-02154396

Submitted on 26 May 2020

Flexibility and Hydration of Amphiphilic Hyperbranched Arabinogalactan-Protein from Plant Exudate: A Volumetric Perspective

Verónica Mejia Tamayo [1], Michaël Nigen [1], Rafael Apolinar-Valiente [2], Thierry Doco [2] , Pascale Williams [2], Denis Renard [3] and Christian Sanchez [1,*]

[1] UMR IATE, UM-INRA-CIRAD-Montpellier Supagro, 2 Place Pierre Viala, F-34060 Montpellier Cedex, France; vero_tati@hotmail.com (V.M.T.); nigen@supagro.inra.fr (M.N.)

[2] UMR SPO, INRA-UM, 2 Place Pierre Viala, F-34060 Montpellier Cedex, France; rafael.apolinar.valient@gmail.com (R.A.-V.); thierry.doco@supagro.inra.fr (T.D.); pascale.williams@supagro.inra.fr (P.W.)

[3] UR1268 Biopolymères Interactions Assemblages, INRA, F-44300 Nantes, France; denis.renard@inra.fr

* Correspondence: christian.sanchez@supagro.inra.fr; Tel.: +33-04-9961-2085

Abstract: Plant Acacia gum exudates are composed by glycosylated hydroxyproline-rich proteins, which have a high proportion of heavily branched neutral and charged sugars in the polysaccharide moiety. These hyperbranched arabinogalactan-proteins (AGP) display a complexity arising from its composition, architecture, and conformation, but also from its polydispersity and capacity to form supramolecular assemblies. Flexibility and hydration partly determined colloidal and interfacial properties of AGPs. In the present article, these parameters were estimated based on measurements of density and sound velocity and the determination of volumetric parameters, e.g., partial specific volume ($v_s°$) and coefficient of partial specific adiabatic compressibility coefficient ($\beta_s°$). Measurements were done with Acacia *senegal*, Acacia *seyal*, and fractions from the former separated according to their hydrophobicity by Hydrophobic Interaction Chromatography, i.e., HIC-F1, HIC-F2, and HIC-F3. Both gums presented close values of $v_s°$ and $\beta_s°$. However, data on fractions suggested a less hydrated and more flexible structure of HIC-F3, in contrast to a less flexible and more hydrated structure of HIC-F2, and especially HIC-F1. The differences between the macromolecular fractions of A. *senegal* are significantly related to the fraction composition, protein/polysaccharide ratio, and type of amino acids and sugars, with a polysaccharide moiety mainly contributing to the global hydrophilicity and a protein part mainly contributing to the global hydrophobicity. These properties form the basis of hydration ability and flexibility of hyperbranched AGP from Acacia gums.

Keywords: acacia gum; partial specific volume; adiabatic compressibility; hydration; flexibility

1. Introduction

Plant Acacia gum exudates from the trunk and branches of Acacia *senegal* and Acacia *seyal* trees are natural viscous fluids that are produced as a protection mechanism of trees [1,2]. Acacia gum exudates are used by humans since prehistoric times for their biological and health beneficial effects, as well as for their transport and interfacial physicochemical properties [2–4]. Acacia gum exudates contain structurally complex biopolymers and minor associated components, such as minerals, traces of lipids and flavonoids, and enzymes [2,4]. Acacia gum biopolymers are highly glycosylated hydroxyproline-rich, arabinogalactan-peptide, and arabinogalactan-proteins that belong to the glycoprotein superfamily [5–7]. Arabinogalactan-proteins (AGPs) have important

biological functions since they are implicated in plant growth, development, signaling, and plant–pathogen interactions [8,9]. AGPs are basically composed of a protein core, which is decorated by arabinose and galactose-rich polysaccharide units with varying amounts of rhamnose, fucose and glucuronic acid [10,11]. Basically, the highly branched polysaccharidic structure consists of 1,3-linked β-D-galactopyranose monomers with side branches that are linked to the main chain mainly through substitution at *O*-6 position. Units of α-L-arabinofuranosyl and α-L-rhamnopyranosyl are distributed in the main and side chains, while β-D-glucuronopyranosyl and 4-*O*-Methyl-β-D-glucuronopyranosyl are mostly end units [12]. In Acacia gums, various populations of hyperbranched AGPs coexist presenting slightly different sugar, amino acid and mineral composition, sugar to amino acid molar ratio, charge density, molar mass, size, shape, and anisotropy [12–22].

When these AGPs are fractionated according to their polarity by hydrophobic interaction chromatography (HIC), three fractions are obtained [13,15]. These fractions have been named in the past: arabinogalactan (AG), arabinogalactan-protein complex (AGP), and glicoproteins (GP), in the order of elution, to take into account their different protein content. However, since all of the fractions react to Yariv's reactant and contain arabinogalactan type II carbohydrate chains, they are formally AGPs. Then, to avoid any possible confusion, these fractions will be more rigorously named, in the order of elution, HIC-F1, HIC-F2, and HIC-F3 in the following. Using a combined experimental approach based on Size exclusion chromatography coupled with multiangle light scattering (SEC-MALS), high resolution microscopic and small angle x-rays scattering (SAXS) and small angle neutron scattering (SANS) experiments, the structure of these fractions was recently considered [17–20]. These studies highlighted common and distinct features between fractions that can be summarized as follows. The sugar composition was closed between fractions, with however larger amount of charged sugars for HIC-F1 and larger amount of arabinose for HIC-F2 and HIC-F3. The amount of proteins increased in the order of polarity, with HIC-F1 < HIC-F2 < HIC-F3 and protein values of about 1%, 8–10% and 20–25%, respectively. All of the fractions were globally composed by three populations of AGPs, low M_w ($M_w < 7.5 \times 10^5$ g·mol^{-1}), high M_w ($M_w > 7.5 \times 10^5$ g·mol^{-1}) and supramolecular assemblies ($M_w > 2$–3×10^6 g·mol^{-1}). Supramolecular assemblies could be structurally self-similar and composed by interacting glycomodules [19,22]. A high amount of low M_w AGP was present in HIC-F1, while high amounts of high M_w AGP and assemblies were found in HIC-F2 and HIC-F3. All of the fractions displayed triaxial ellipsidal shapes, with varying semi axis dimensions and anisotropies. Low M_w AGPs were in general more spheroidal and less anisotropic than the larger ones. HIC-F1 displayed an inner dense branched structure, while HIC-F2, but especially HIC-F3, were more porous and expanded. Because of the presence of charged sugars and amino acids, all fractions were negatively charged with weak polyelectrolyte behavior. The solvent affinity of fractions, estimated from the inverse of the power-law exponent describing the intermediate q range of small angle scattering form factor, or alternatively by the exponent of the relationships between M_w and the intrinsic viscosity, coherently indicated that the solvent affinity of HIC fractions were intermediate between a poor affinity (0.33) and a good one (0.6).

This short summary points out that the complexity of plant exudates not only comes from the complex composition and architecture of individual AGPs, but also from the structural and physicochemical polydispersity, reinforced by interactions between macromolecules that induce the formation of supramolecular structures [10,15,18–20,23–27]. Apprehending this complexity is needed in order to better understand the physicochemical properties of AGPs from plant exudates, especially solubility and interfacial properties, which ultimately determine the practical use of gums in confectionaries, soft drinks and adhesive- or coating-based applications. In general, solubility and interfacial properties of biopolymers are determined both by intrinsic properties of macromolecules (composition, accessibility, and spatial division of charged, polar and nonpolar atomic groups, chain density, molar mass, conformation, flexibility) and their ability to dynamically interact with the solvent. Many of their general dynamic properties can be described in terms of bulk quantities, for instance packing density, compressibility, or other coefficients of elasticity, which are typically applied to

macroscopic systems [28]. Volumetric properties of biopolymers are directly related to their flexibility and hydration, then providing a convenient mean to assess these important molecular characteristics. In particular, the partial molar volume, V_s° and the partial molar adiabatic compressibility, K_s°, are macroscopic thermodynamic observables that are particularly sensitive to the hydration properties of solvent exposed atomic groups, as well as to the structure, dynamics, and conformational properties of the solvent inaccessible biopolymer interior [29,30]. This has motivated many efforts to experimentally measure these quantities on small solutes (amino acids, sugars, minerals) and on biopolymers, such as globular, fibrous, and unfolded proteins [31–40], nucleic acids [33,35,41–43] and linear or branched polysaccharides [33,44–54].

In the present article, we reported the volumetric experimental characterization of hyperbranched charged AGPs from Acacia gums. Specific objectives of the work were to qualitatively estimate the molecular flexibility of hyperbranched AGPs and their hydration ability. We characterized the two classically used total gums, i.e., Acacia *senegal* and Acacia *seyal* gums, and the three HIC fractions that were isolated from the former. Following a detailed analysis of volumetric data obtained on fractions, we estimated the flexibility and hydration characteristics of the three fractions of AGPs in dilute solutions. The results of the analysis shed light to the importance of the sugar composition and protein content on the hydration ability of AGPs, but also on the intrinsic spatial structural heterogeneity, which determines macromolecular volume fluctuations, and therefore, the molecular flexibility.

2. Materials and Methods

2.1. Materials

The experiments were carried out using commercially available Acacia *senegal* (A. *senegal*, lots OF 110676 and OF 152413) and Acacia *seyal* (A. *seyal*, lot OF 110724) soluble powders, kindly provided by the Alland & Robert Company—Natural and Organic gums (Port Mort, France). The moisture, sugar, and mineral content of the powders were previously reported elsewhere [21].

All of the reagents used were of analytical grade from Sigma Aldrich (St. Louis, MO, USA).

2.2. Methods

2.2.1. Chemical Analyses

Moisture and ash contents of Acacia gum and HIC fraction samples were analyzed by the Hot Air Oven and Gravimetric methods (AOAC 925.10 and AOAC 923.03, respectively). Amino acid, neutral sugars, and uronic acid compositions were determined as reported in Lopez et al. [21]. Measures were duplicated.

2.2.2. Desalting of Acacia Gums and HIC Fractions

Acacia gum samples were prepared from a 10% (*w/w*) dispersion of commercial A. *senegal* and A. *seyal* powders in ultrapure deionized water (18.2 mΩ). Dispersions were stirred overnight at room temperature (20–25 °C) to allow for the complete hydration of Acacia gum molecules, followed by centrifugation at 12,000 rpm (20 °C) for 30 min to remove impurities. Dispersions were desalted by diafiltration against deionized water (18.2 mΩ) using a 1:3 (*v/v*) AG:water volume ratio, using an AKTA FLUX 6 system (GE Healthcare, Upsala, Sweden), with a transmembrane pressure of 15 psi. The membrane used was a Polysulfone Hollow fiber (GE Healthcare) with a nominal cut off of 30 kDa (63.5 cm L × 3.2 cm o.d., surface of 4800 cm^2). The sample was then centrifuged at 12,000 rpm (20 °C) for 30 min and freeze-dried for 72 h.

Macromolecular fractions, HIC-F1, HIC-F2, and HIC-F3 were obtained from A. *senegal* soluble powder via Hydrophobic Interaction Chromatography (HIC), according to the classical fractionation method that was used by Randall et al. [13] and Renard et al. [15]. HIC-F1 and HIC-F2 followed

the same diafiltration procedure as A. *senegal*, and were then spray dried. The HIC-F3 fraction was concentrated using a rotavapor (until crystals appeared), extensively dialyzed (72 h), and freeze dried (72 h). The HIC-F3 fraction could not be desalted by dialfiltration because of excessive material losses during the process. Please note that freeze-drying of HIC-F3 was controlled to reach final sample moisture not below 10%. Otherwise, about 50% of macromolecules become insoluble upon rehydration, as noted elsewhere [15,23].

2.2.3. Preparation of Acacia Gum Dispersions

Acacia gums and HIC fraction powders were dispersed and dialyzed against the solvent under constant agitation overnight at room temperature (1:5 AG:solvent volume ratio, 3.5 KDa Spectra/Por membrane) to reach isopotential equilibrium. Dispersions were centrifuged at 12,000 rpm (20 °C) for 30 min to remove impurities and degassed for 15 min to remove dissolved air (300 Ultrasonik bath, Ney, Yucaipa, CA, USA). The dialyzed solvent was used as reference in volumetric measurements.

The concentrations of Acacia gums and HIC fractions in dispersions were quantified using an Abbemat Refractometer (Anton Paar, Graz, Austria) and experimental refractive index increments (dn/dc) of 0.155, 0.151, 0.162, 0.160, and 0.145 mL·g^{-1} for A. *senegal*, A. *seyal*, HIC-F1, HIC-F2, and HIC-F3, respectively. The repeatability of the instrument is 1×10^{-6}. All of the measurements were performed at 25 °C and triplicated.

2.2.4. Size Exclusion Chromatography (HPSEC)-Multi Angle Light Scattering (MALS)

Acacia gums and HIC fractions were characterized by multi-detector high performance size exclusion chromatography (HPSEC). HPSEC experiments were performed using a Shimadzu HPLC system (Shimadzu, Kyoto, Japan) coupled to four detectors: a Multi Angle Light Scattering detector which operates at 18 angles (DAWN Heleos II, Wyatt, Santa Barbara, CA, USA), a differential refractometer (Optilab T-rEX, Wyatt, Santa Barbara, CA, USA), an on line Viscosimeter (VISCOSTAR II, Wyatt, Santa Barbara, CA, USA), and a UV VIS detector activated at 280 nm (SPD-20A, Shimadzu). The separation of macromolecules was performed on a column system composed of one Shodex OHPAK SB-G pre-column followed by four columns in series (SHODEX OHPAK SB 803 HQ, SB 804 HQ, SB 805 HQ, and OHPAK SB 806 HQ) for A. gums and HIC-F1 fraction, and 1 column (SHODEX OHPAK SB 805 HQ) for HIC-F2 and HIC-F3 fractions.

Acacia gums and HIC fractions based dispersions (1 mg·cm^{-3}) were injected and eluted using 0.1 M LiNO$_3$ (0.02% NaN$_3$) at 1 cm^3·min^{-1} and 30 °C. The data were analyzed using the dn/dc mentioned in the upper section and ASTRA software 6.1.2.84 (Wyatt Technologies, Santa Barbara, CA, USA).

2.2.5. Density and Sound Velocity Measurements

Density and sound velocity of Acacia gum solutions were simultaneously determined at 25 °C using a DSA 5000M sonodensimeter (Anton Paar, France). The instrument is equipped with a density cell and a sound velocity cell, the repeatability was 1×10^{-6} g·cm^{-3} for density, and 0.1 m·s^{-1} for sound velocity. Measurements were triplicated. Averaged volumetric parameters were determined from the ensemble of measured points. Measurements were done on samples described above, but also on additional samples not discussed in details in this paper, for instance, arabic acid that was obtained from A. *senegal* gum upon acidification and extensive demineralization, and other AGP fractions stemming from various runs of classical hydrophobic interaction and/or ion-exchange chromatographies.

2.3. Theoretical Treatment of Density and Sound Velocity Parameters

2.3.1. Partial Specific Volume

The partial specific volume ($v_s°$) of a solute is defined as the change on the volume (V) of the system that was caused by the addition of an infinitesimal amount of the solute at constant pressure (P) and temperature (T) provided that the amount of the solvent (m_j) is kept constant (Equation (1)) [33,55,56].

$$v_s° = \left(\frac{\partial V}{\partial m_i} \right)_{P,T,m_j}, \ (i \neq j) \tag{1}$$

Literature suggests two methods to obtain $v_s°$, the slope and the extrapolation [56]. The first one is used mainly in dispersions where the differences between the density of solute and solution are important (Equation (2)). The second one uses the apparent volume of dispersions (Equation (3)), since in highly diluted conditions apparent and partial specific volumes are similar [32,33,55–58].

$$v_s° = \frac{1}{\rho_o} \left(1 - \frac{\rho - \rho_o}{C} \right) \tag{2}$$

where: ρ_o and ρ are the density of the solvent and dispersion, respectively, and C is the concentration of the solute.

$$v_s° = \frac{1}{\rho_o} \lim_{c \to 0} \frac{\rho - \rho_o}{C} \tag{3}$$

In order to determine $v_s°$, the intramolecular interactions between solute molecules have to be negligible. Furthermore, its value depends on the concentration range studied. For Acacia gums and HIC fraction dispersions, $v_s°$ was determined using the slope method in a range of concentrations between 20 and 70 g·L^{-1}, where repeatability and reproducibility of assays were reliable. Unpredictable variation of results was observed at gum concentrations below 20 g·L^{-1}, due mainly to interaction and aggregation phenomena.

2.3.2. Isoentropic Compressibility Coefficients

The adiabatic compressibility of the solute (K_s) is defined as the first derivative of the volume of the system with respect to its pressure at constant entropy (S) (Equation (4)) [59]. It represents the apparent adiabatic compressibility (β_s) that is caused by addition of an infinitesimal amount of the solute.

$$K_s = \beta_s V = -\left(\frac{\partial V}{\partial P} \right)_S \tag{4}$$

The adiabatic compressibility coefficient of the dispersion is related to the sound velocity by the Newton Laplace equation (Equation (5)).

$$\beta°_s = -\left(\frac{1}{V} \right) \left(\frac{\partial V}{\partial P} \right)_S = \frac{1}{\rho u^2} \tag{5}$$

where: u is the sound velocity of the dispersion and ρ is the density of the solution. The partial specific adiabatic compressibility coefficient ($\beta_s°$) can be calculated from density and sound velocity measurements, using the following expression [49,50,56,60]:

$$\beta°_s = \left(\frac{\beta_{so}}{v_s°} \right) \lim_{c \to 0} \left[\frac{\beta / \beta_{so} - \Phi}{C} \right] \tag{6}$$

where: β and β$_{so}$ are the adiabatic compressibilities of the dispersion and solvent, respectively, and, Φ is the apparent specific volume (Φ = (ρ − C)/ρ$_o$).

2.3.3. Microscopic Description of Macroscopic Volumetric Data

In order to interpret less qualitatively macroscopic data in terms of microscopic phenomena, one need to separate each macroscopic variable into contributing components that can be ascribed to specific molecular "events" [29]. This can be done using the scaled particle theory that describes the process of introducing a solute molecule into a solvent according to two steps [61–64]. The first corresponds to the creation of a cavity into the solvent able to accommodate the solute. The second is the introduction into the cavity of a solute molecule that interacts with the solvent. In terms of partial molar volumes, this can be described according to [63,65]:

$$\overline{V}_s^\circ = \overline{V}_c + \overline{V}_l + \beta_{T0}RT \tag{7}$$

where $\overline{V}_s^\circ$ is the partial molar volume of the solute at infinite dilution, $\overline{V}_c$ is the partial molar volume change upon cavity formation, $\overline{V}_l$ is the partial molar volume change upon interactions of charged, polar, and nonpolar atomic groups with the solvent (interaction volume), β_{T0} is the coefficient of isothermal compressibility of the solvent and RT is the energy of ideal gases. The term $\beta_{T0}RT$ is the ideal component of the partial molar volume resulting from the motion of the solute along the translational degrees of freedom. This parameter is small (about 1.1 cm$^3\cdot$mol^{-1} at 25 °C) and can be neglected [64], especially in the case of biopolymers, such as globular proteins or polysaccharides where the partial molar volumes are larger than ≈10^4–10^5 cm$^3\cdot$mol^{-1} [32,54]. Omitting for simplicity the bars onto the volume terms, the equation can be described as [29,38,63,64,66,67]:

$$V_s^\circ = V_c + V_l = V_M + V_T + V_l \tag{8}$$

$$V_s^\circ = V_{vdW} + V_{void} + V_T + n_h \left(V_h^\circ - V_o^\circ \right) \tag{9}$$

where $V_M = (V_{vdW} + V_{void})$ is the intrinsic partial molar volume of the solute, which corresponds to the spatial architecture of protein interior [59], a domain where water cannot penetrate, V_{vdW} is the van der Waals partial molar volume of the solute and V_{void} is the partial molar volume of voids into the solute due to imperfect atom packing; V_T is the partial molar thermal volume that represents an "empty volume" around the solute molecules resulting from thermally induced mutual molecular vibrations and reorientations of the solute and the solvent [63,68,69]. It is related to the fact that the "cavity" of the solute molecule that is created by inserting the molecule into the solvent should be larger than its molecular volume, and this extra volume should be sensitive to temperature [38,69]. For molecules of arbitrary shapes, the thermal volume can be approximated as a layer of constant thickness Δ to the surface of the molecule [64]; and, V_l the interaction volume is equal to $n_h \left(V_h^\circ - V_o^\circ \right)$, with n_h the hydration number, i.e., the number of water molecules that are involved in the solute hydration shell, and V_h° and V_o° the partial molar volumes of water in the hydration shell and in the bulk state, respectively [29]. The term hydration shell refers to those water molecules, which is due to the presence of the solute exhibiting altered physicochemical characteristics when compared with bulk water [37]. V_l is the only term sensitive to hydration and its contribution is negative because $V_h^\circ < V_o^\circ$.

Regarding the partial molar adiabatic compressibility K_s°, the relationship is [36,37,70]:

$$K_s^\circ = K_M + n_h \left(K_{sh}^\circ - K_{so}^\circ \right) + K_r \tag{9}$$

where K_M is the intrinsic partial molar adiabatic compressibility of the solute, n_h is the hydration number, K_{sh}°, and K_{so}° are the partial molar adiabatic compressibility of water in the hydration shell and bulk water, respectively, and K_r is a relaxation component that results from the redistribution of

biopolymer conformational sub-states due to pressure and temperature variations in the field of the ultrasonic waves [37]. The term K_M is proportional to the partial molar volume V_M, according to [29]:

$$K_M = \beta_M V_M \tag{10}$$

where β_M is the coefficient of adiabatic compressibility of the biopolymer interior. This term is a measure of intra-macromolecular interactions that can be calculated from:

$$\beta_M = B_M \frac{V_M}{V_{vdW}} \tag{11}$$

where B_M is the coefficient of proportionality and $\frac{V_M}{V_{vdW}}$ is inverse of the molecular packing density ρ_M [29,41].

It is important to note from the two above equations that the values of the apparent molar volume and the apparent molar adiabatic compressibility of a solute are sensitive to both the intrinsic molecular characteristics of solutes, and the quantity and the quality of hydration. The quantity of hydration corresponds to the amount of solvating water molecules in the hydration shell (n_h). On the other hand, the quality of hydration is reflected in the values of the partial molar volume, V_h° and the partial molar adiabatic compressibility, K_{sh}°, of the hydration water, which inform on the ability of charged, polar, and nonpolar chemical groups to alter its structure and physicochemical properties [35,37,63,71]. In other words, n_h indicates how much water molecules are perturbed by the solute, and V_h° and K_{sh}° indicate how strong is the water molecule solute interaction.

3. Results

3.1. Theoretical Treatment of Density and Sound Velocity Parameters

The global biochemical composition of A. *seyal* and A. *senegal* gums and HIC fractions obtained from the latter, i.e., HIC-F1, HIC-F3 and HIC-F3 is presented in Table 1. Classically, all of the AGPs from A. gums were composed of the same sugars: D-galactose, L-arabinose, Rhamnose, D-glucuronic acid and 4-O-methyl glucuronic acid, galactose and arabinose being the main sugars present [4,13–15,21,72,73]. The molar ratio of Arabinose to Galactose (Ara/Gal) of A. *senegal* and A. *seyal* was 0.8 and 1.4, respectively. Meanwhile, the Ara/Gal ratio of A. *senegal* fractions was 0.69, 1.04 and 1.15 for HIC-F1, HIC-F2, and HIC-F3, respectively. These results were close to previously reported values for A. *senegal* fractions: 0.57 [15] and 1.25 [13] for HIC-F1; 0.75 [15] and 0.93 [13] for HIC-F2; and, 0.76 [15] and 0.82 [13] for HIC-F3. The three fractions have a similar amount of neutral sugars (Ara, Gal and Rha), however HIC-F1 has a higher uronic acid to neutral sugar ratio (0.28), as compared to HIC-F2 and HIC-F3 (0.19 and 0.17, respectively). A consequence is that the carbohydrate moiety of HIC-F1 is supposed to carry more negative charges than HIC-F3. This difference in charge density between HIC-fractions is certainly exacerbated by the difference in mineral contents between fractions. In particular, within fractions, HIC-F3 contained the larger amount of minerals (5%), which can be due both to difference in the applied demineralization treatment (see Section 2) and to the higher content in aspartic and glutamic amino acid residues (13.5%, 9.6% and 5.7% for HIC-F3, HIC-F2, and HIC-F1, respectively).

As expected, HIC-F3 showed a higher amount of proteins (14%) as compared to HIC-F1 (0.5%) and HIC-F2 (6.3%). These protein content, as determined twice by the Kjeldhal method and close to that estimated from amino acid analysis (results not shown), were approximatively two times lower than values determined previously [15]. Likely, extensive desalting of fractions and losses of some protein rich AGP species during the semi-preparative fractionation could explain this discrepancy. This also suggests that part of proteins could be not associated with the protein core of AGPs, but free. The amino acid composition of Acacia gums and HIC fractions is presented in Supplementary Table S1. All of the gums showed a similar amino acid profile. As is common for most AGPs, hydroxyproline and

serine are the dominant amino acids, with an also significant amount of proline, threonine, histidine, and leucine, which is in good agreement with the literature [4,13–15,21,75,76]. We also remarked that glutamic and aspartic acid amino acids are important with summed values of 10.1, 10.8, 5.7, 9.6, 13.5 for, respectively, A. *senegal*, A. *seyal*, HIC-F1, HIC-F2, and HIC-F3. A main difference between the fractions is then the content of negatively-charged amino acids. Another difference is the higher Hyp content of HIC-F1 fraction (36.4%) as compared to HIC-F2 (28.8%) and HIC-F3 (19.2%). Importantly, HIC-F1 contained about 81% of polar and charged amino acids while this value was smaller for HIC-F2 (73%) and HIC-F3 (68%). The presence of only 19 to 32% of nonpolar amino acids in HIC fractions seriously questions the current view of AGPs as kind of Janus biopolymers with a hydrophilic sugar moiety and a hydrophobic protein moiety. The subject is beyond the scope of the present article, however clustering of nonpolar amino acids in terminal regions of polypeptides, the presence of secondary structures, weak energy interactions between amino acids and sugars in close proximity, amphiphilic helix-type structures of the galactan backbone, and associative properties of macromolecules, all of these characteristics must play a role in the subtle balance between polar and nonpolar properties of AGPs [15,20,77,78]. Nevertheless, due mainly to the higher protein content and percentage in nonpolar amino acids, HIC-F3 fraction is the less polar one.

Table 1. Biochemical composition of Acacia gums and hydrophobic interaction chromatography (HIC) fractions in dry basis (mean ± standard deviation).

Component (mg·g^{-1})	A. *senegal*	HIC-F1	HIC-F2	HIC-F3	A. *seyal*
Total Dry Matter	893.4 ± 4.0	921.6 ± 0.1	926.2 ± 1.0	921.9 ± 2.0	966.9 ± 2.5
Sugars [a]	944.4	961.3	918.3	813.0	978.0
Arabinose (%) [b]	30.2 ± 0.6	26.8 ± 1.3	35.6 ± 1.0	38.3 ± 2.1	48.5 ± 1.7
Galactose (%) [b]	40.5 ± 1.7	39.0 ± 0.8	34.4 ± 0.8	33.3 ± 1.8	34.2 ± 2.0
Rhamnose (%) [b]	12.4 ± 0.4	12.5 ± 0.1	13.7 ± 0.4	13.9 ± 1.0	3.2 ± 0.7
Glucuronic Acid (%) [b]	17.8 ± 1.7	20.3 ± 0.6	15.6 ± 0.6	13.7 ± 2.1	7.7 ± 0.4
4-*O*-Me-Glucuronic Acid (%) [b]	1.0 ± 0.1	1.4 ± 0.1	0.6 ± 0.1	0.7 ± 0.1	6.4 ± 0.6
Branching degree [d]	0.78	0.77	0.75	0.75	0.59
Proteins [c]	21.5 ± 0.9	4.9 ± 0.1	63.1 ± 1.2	137.7 ± 2.7	7.7 ± 0.0
	(27) [e]	(19) [e]	(27) [e]	(32) [e]	(29) [e]
Minerals	34.1 ± 0.1	30.5 ± 1.1	19.3 ± 1.1	49.3 ± 2.6	14.3 ± 2.5

[a] Total content of sugars calculated from the difference of proteins and minerals from 1000 mg·g^{-1}. [b] Sugar composition was determined by GC-MS. [c] Protein content was measured using the Kjeldhal method. [d] determined on neutral sugars according to the equation DB = 2D/(2D + L), where D is the number of dendritic units or branched units linked at three or more sites and L is the number of linear units having two glycosidic linkages [21,74]. [e] Percentage in nonpolar amino acids.

In terms of basic structural parameters, A. *senegal* showed lower M_w (6.8×10^5 g·mol^{-1}) than A. *seyal* (7.1×10^5 g·mol^{-1}) but a larger polydispersity index (M_w/M_n) (Table 2). In addition, A. *seyal* displayed a smaller intrinsic viscosity than A. *senegal*, then a smaller hydrodynamic volume, indicating a more compact conformation of the former. Comparable results are reported in literature [15,21,24,73,79,80]. Regarding the HIC fractions, HIC-F1, HIC-F2, and HIC-F3 showed M_w of 3.5×10^5, 1.5×10^6, and 1.6×10^6 g·mol^{-1}, respectively, as already reported [15]. The polydispersity index of HIC-F3 was higher (1.9) when compared to HIC-F1 and HIC-F2 (1.4 and 1.3, respectively). On the other hand, the density of fractions was not identical with a density decreasing in the order HIC-F1 > HIC-F2 > HIC-F3.

Combining biochemical composition and structural parameters allowed for deducing or calculating a number of basic parameters, both for the polysaccharide and peptide/protein moieties that will be used in the following (Table 3).

Table 2. Structural parameters of Acacia gums and HIC fractions in aqueous solutions (1 g·L^{-1} at pH 5) obtained by high performance size exclusion chromatography (HPSEC)-Multi Angle Light Scattering (MALS).

	A. senegal	HIC-F1	HIC-F2	HIC-F3	*A. seyal*
M_w (g·mol^{-1})	6.8×10^5	3.5×10^5	1.5×10^6	1.6×10^6	7.1×10^5
M_n (g·mol^{-1})	3.1×10^5	2.3×10^5	1.1×10^6	9.0×10^5	4.2×10^5
M_w/M_n	2.0	1.4	1.3	1.9	1.5
$M_w < 7.5 \times 10^5$ g·mol^{-1} (%)	86	93.0	12.3	22.7	80
$M_w > 7.5 \times 10^5$ g·mol^{-1} (%)	14	7.0	87.7	67.3	20
Density (g·cm^{-3})	0.99766	0.99775	0.99759	0.99743	0.99747

Table 3. Basic composition and structural parameters of Acacia gums and HIC fractions in aqueous solutions (1 g·L^{-1} at pH 5) as obtained from chemical analyses and HPSEC-MALS measurements.

Basic Molecular Characteristics	HIC-F1	HIC-F2	HIC-F3
AGP M_w (g·mol^{-1})	348,300	1,495,000	1,643,000
Polysaccharide moiety M_w (g·mol^{-1})	346,593	1,400,666	1,416,759
Average sugar residue M_w (g·mol^{-1})	173.2	169.3	168.2
Average sugar partial molar volume (cm^3·mol^{-1})	105.9	104.3	103.9
Average sugar van der Waals volume (Å^3)	136.9	133.8	133.0
Number of sugar residues	2001	8441	9375
Potential number of charged and polar interacting sites (Polysaccharide moiety)	6273	29,183	28,789
Protein moiety M_w (g·mol^{-1})	1707	94,335	226,241
Average aminoacid residue M_w (g·mol^{-1})	127.3	128.2	129.5
Number of aminoacid residues	13	736	1747
Charged and polar aminoacids (%)	80	72	67
Hydrophobicity index [a]	-1.46	-1.01	-1.14
Potential number of charged and polar interacting sites (Protein moiety)	12	621	1391

[a] from the hydrophobicity scale proposed by Zhu et al. [81].

3.2. Volumetric Properties

The partial specific volume, v_s°, partial specific adiabatic compressibility, $k_s^\circ = (\beta_s^\circ / v_s^\circ)$, and coefficient of partial specific adiabatic compressibility, β°, of A. *seyal*, A. *senegal* and its HIC fractions are presented in Table 4. It is first noteworthy that all of the obtained k_s° or β_s° values were negative, which indicates that the hydration contribution is more important than the intrinsic contribution for the entire population of AGPs [29,32,36,60]. For A. *senegal*, experiments were done at pH 5, in water, sodium acetate buffer 10 mM, and LiNO$_3$ 100 mM. We did not remark an important effect of ionic strength. Thus, for instance, v_s° and β_s° were, respectively, in the range 0.5842–0.5940 cm^3·g^{-1} and -12.0×10^{-11}–12.3×10^{-11} Pa^{-1} (Table 4). We however noted that v_s° was larger in LiNO$_3$ 100 mM (0.5940), suggesting a decrease of macromolecule hydration through partial shielding of charges. Hydration has a negative contribution on global volume because the v_s° of water molecules interacting with a solute is lower than that of bulk water. More globally, these results would indicate that the solvent ionic strength has little effect on the measured volumetric properties of A. *senegal*, according to our experimental conditions. Regarding both total Acacia gums, A. *seyal* displayed in acetate buffer 10 mM smaller partial specific volume v_s° than A. *senegal* (0.5767 vs. 0.5842 cm^3·g^{-1}) and more negative β_s° value (-13.2 vs. -12.2 Pa^{-1}) (Table 4). This indicated that A. *seyal* was more hydrated in solution than A. *senegal*, despite a smaller content in charged sugars (Table 1). Possible reasons for these differences may be the larger mineral and protein content of A. *senegal* gum, but also the higher arabinose content of A. *seyal*. Higher arabinose content promotes the formation of long linear arabinose chains that display important hydration properties [21]. Literature reported values of v_s° of 0.60–0.62 cm^3·g^{-1} and β_s° around 10^{-11}–10^{-10} Pa^{-1} for neutral unmodified sugars, such as galactose and arabinose [33,36,56,82–84], which are the main sugars present in AGPs

from Acacia gums. Additionally, values of v_s° and β_s° around 0.61–0.62 cm$^3 \cdot$g^{-1} and -3.5×10^{-11} to -16.4×10^{-11} Pa^{-1} have been reported for branched polysaccharides, such as dextran and oligodextran of different M_w at 25 °C [47,49–52]. Besides, v_s° values ranging from 0.40 to 0.553 cm$^3 \cdot$g^{-1} and β_s° of -20×10^{-11} to -70×10^{-11} Pa^{-1} have been reported for modified dextran (SPD, DS, and CMD) of different M_w [50] and linear polysaccharides, such as carragenans [54] and hyaluronate potassium salt [48]. Our experimental values are therefore in good agreement with the literature.

Table 4. Partial specific volume (v_s°, cm$^3 \cdot$g^{-1}), partial specific adiabatic compressibility (k_s°, cm$^3 \cdot$g$^{-1} \cdot$Pa^{-1}) and coefficient of partial specific adiabatic compressibility (β_s°, Pa^{-1}) obtained for A. *seyal* gum, A. *senegal* gum and its fractions HIC-F1, HIC-F2 and HIC-F3. All measurements were done at 25 °C using pH 5 acetate buffer 10 mM unless specified in the table. HIC: Hydrophobic Interactions Chromatography.

Type of Acacia Gum or Fraction	v_s° (cm$^3 \cdot$g^{-1})	k_s° ($10^{11} \times$ cm$^3 \cdot$g$^{-1} \cdot$Pa^{-1})	β_s° ($10^{11} \times$ Pa^{-1})
A. *seyal*	0.5767	−7.6	−13.2
A. *senegal* [a]	0.5870	−7.2	−12.2
A. *senegal*	0.5842	−7.1	−12.2
A. *senegal* [b]	0.5940	−7.5	−12.5
A. *Senegal* [c]	0.5880	−7.3	−12.3
A. *Senegal* [d]	0.5850	−7.0	−12.0
HIC-F1	0.5616	−10.3	−18.3
HIC-F2	0.5876	−8.5	−14.4
HIC-F3	0.6500	−0.7	−1.0

[a] solvent: H$_2$O; [b] solvent: LiNO$_3$ 100 mM; [c] desalted A. *senegal* (2.1% minerals); [d] dialyzed A. *senegal* (3.3% minerals).

If volumetric parameters were close for total Acacia gums (A. *senegal* and A. *seyal*), then the situation was clearly different for HIC fractions from A. *senegal*. In this case, both v_s° and β_s° increased (became less negative for β_s°) from HIC-F1 to HIC-F3. These results show the clear effect of the differences in fraction biochemical composition, but especially of AGP hydrophobicity on volumetric properties, as results have already demonstrated for globular proteins [32]. As HIC-F1 the most polar AGP, according to its HIC elution order and protein content, it will be able to bind more water molecules, and therefore will have a more hydrated and less flexible structure than HIC-F2 and HIC-F3. Conversely, HIC-F3 will have in theory a less hydrated and more flexible structure, as will be demonstrated in the discussion section. The increase of the v_s° parameter in the fractions was apparently strongly correlated to the protein content since we know that the v_s° of polysaccharides and globular proteins is in average, respectively, of around 0.60 and 0.72 cm$^3 \cdot$g^{-1} [29,32,33]. The effect of AGP protein content on v_s° can be seen in Figure 1, where data for total Acacia gums and HIC fractions, but also for other modified gum (arabic acid) and other batches from hydrophobic interaction chromatography or ion-exchange chromatography have been shown. Interestingly, data for AGP formed a continuity from literature data obtained on glycoproteins containing from 7 to 98% proteins [85], suggesting the view that in solution, volumetric properties of AGP from Acacia gums are strongly (directly and indirectly) determined by their protein content.
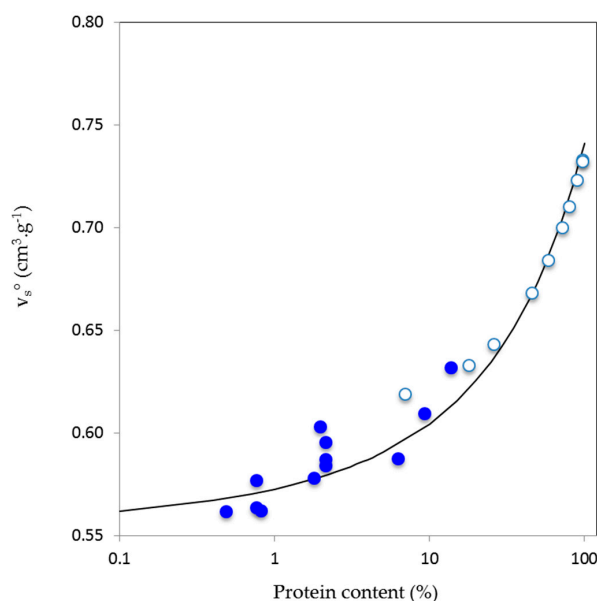
Figure 1. Effect of protein content on the partial specific volume (v_s°, cm$^3 \cdot$g^{-1}) of Acacia gums (A. *senegal* and A. *seyal*), arabic acid and various molecular fractions (see Section 2) obtained from A. *senegal* gum by hydrophobic interaction chromatography or ion-exchange chromatography (blue circles) and various glycoproteins containing from 7 to 98% of proteins [85] (white circles). Continuous line is a guide to the eye (equation $v_s^\circ = 0.545 + 0.012\exp([\text{protein}]^{0.222})$).

4. Discussion

Hyperbranched AGPs from Acacia gums are structured macromolecules containing a protein core onto which massive sugar blocks and more linear sugar chains are connected [4]. Sugars are mainly neutral, however charged sugars and some amino acid residues contribute with charges that are at the basis of the polyectrolyte nature of AGPs. Polar and charged residues provide hydrophilic properties to AGPs that are balanced by the nonpolar characteristics of about 20–30% of amino acids and the presence of methyl groups on rhamnose and 4-*O*-methyl glucuronic acids. The hydrophobicity of AGPs comes directly from their chemical composition, but also through their structural organization since both the polysaccharide and protein moieties contain a number of secondary structures (α and PPII helices, β-sheet structures, and turns) with specific hydrophilic/hydrophobic balances. Composition and structure of AGPs determine their behavior in solution, especially their flexibility and hydration, which can be approached through measurements of their volumetric properties. Volumetric parameters that were measured on A. *seyal*, A. *senegal* and its HIC fractions, i.e., partial specific volume, v_s°, and coefficient of partial specific adiabatic compressibility, β_s°, indicated that the protein content of AGPs was an important parameter and that hydration of macromolecules (negative values of β_s°) was in absolute value larger than the intrinsic compressibility (flexibility) contribution. In order to get a more general view of the volumetric behavior of AGPs, we then compared it to those of proteins and polysaccharides that we took from the literature [29,32,48,49,52,54,57,86]. Polysaccharides are charged linear polysaccharides salts (K- and Na-carageenans, K-hyaluronate) or branched dextran derivatives (sulfate-, sulfopropyl- and carboxymethyl dextrans) and neutral dextrans (various M_w). We also considered volumetric data obtained with nucleic acids [42,87]. For AGPs, we use data from total Acacia gums (A. *senegal* and *seyal*) and AGP fractions (Table 4), and additional data not specifically discussed in this paper, for instance, arabic acid obtained from A. *senegal* gum upon acidification and extensive demineralization, and other AGP fractions stemming from various runs of classical hydrophobic interaction and/or ion-exchange chromatographies. Figure 2 shows the coefficient of partial specific adiabatic compressibility $\beta_s^\circ = k_s^\circ / v_s^\circ$ (Pa^{-1}) as a function of partial specific volume $v_s^\circ = \left(V_s^\circ / M_w \right)$ (cm$^3 \cdot$g^{-1}).

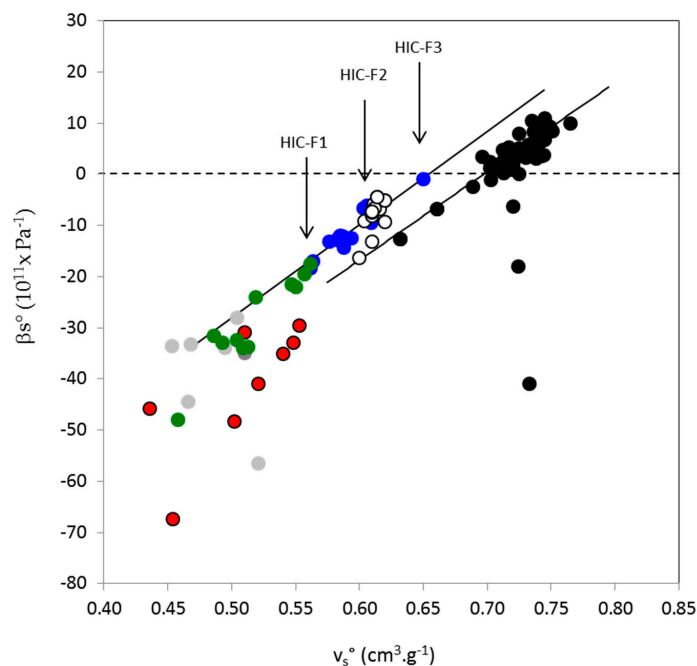**Figure 2.** Relationship at 25 °C between the partial specific volume ($v_s°$, $cm^3 \cdot g^{-1}$) and the coefficient of partial specific adiabatic compressibility ($\beta_s°$, Pa^{-1}) for Acacia gums (A. *senegal* and A. *seyal*), arabic acid and various molecular fractions (see Section 2) obtained from A. *senegal* gum by hydrophobic interaction chromatography or ion-exchange chromatography (blue circles), various polysaccharides (neutral dextrans, white circles; charged dextran derivatives, red circles); Na- and K-carageenans, light gray circles, K hyaluronate, dark gray circle), various nucleic acids (green circle) and various globular proteins (black circles). Density and sound speed were measured in pH 5 acetate buffer for arabinogalactan-proteins (AGP). Vertical arrows point out HIC-F1 (left), HIC-F2 and HIC-F3 (right) fractions. Continuous lines are linear regressions with equations ($\beta_s° = 185 \times v_s° - 129$) and ($\beta_s° = 195 \times v_s° - 127$) for globular proteins and AGPs, respectively.

A roughly linear tendency exists between $\beta_s°$ and $v_s°$ on the ensemble of data, with k_s^0 increasing with the increase of $v_s°$, as expected from the positive contribution of volume fluctuations (intrinsic flexibility) and the negative contribution of hydration [29,32,41]. The relationship between $\beta_s°$ and $v_s°$ could then be considered as a polarity-flexibility qualitative scale [32,41], delimiting three biopolymer groups from the highly polar and rigid charged polysaccharides and nucleic acids ($\beta_s° < -20 \times 10^{-11}$ Pa^{-1}; $v_s° < 0.56$ $cm^3 \cdot g^{-1}$) to the less polar and more flexible globular proteins ($\beta_s°$ essentially positive; $v_s° > 0.7$ $cm^3 \cdot g^{-1}$), as noted in Gekko and Hasegawa [32]. In this virtual polarity-flexibility scale of biopolymers, AGP then display an intermediate behavior. Accordingly, fractions containing a larger amount of polysaccharides (HIC-F1; 97% polysaccharide, 0.5% protein) and less hydrophobic, according to the principle of the used separation technique, are closer to the linear and charged branched polysaccharides and nucleic acids (more hydration, lower flexibility), while fractions that are richer in protein (HIC-F3; 81 wt% polysaccharide, 14 wt% protein) and more hydrophobic, are closer to the protein group (lower hydration, larger flexibility), with a $\beta_s°$ value close to zero. This observation suggested again that hydration of fractions decreases in the order HIC-F3 < HIC-F2 < HIC-F1, a point that is confirmed in the next section. The fact that AGP data were close to those obtained for neutral dextrans, in line with a moderate hydration and flexibility of AGPs, demonstrates the weak polyelectrolyte characteristics of AGPs from Acacia gums [88]. These characteristics can explain that A. *senegal* gums dissolved in solvents of distinct ionic strengths or dissolved in the same solvent (pH 5 sodium acetate buffer), but containing different salt concentrations, display close $\beta_s°$ and $v_s°$ parameters (see Table 4). Finally, we determined for AGP data the linear relationship between $\beta_s°$ and $v_s°$ and we found an equation $\beta_s° \approx 185 \times v_s° - 129$ (R^2:0.93) that

was closed to that obtained with a great number of globular proteins ($\beta_s^o \approx 195 \times v_s^o - 127$, R^2:0.85) [32]. We do not think that this result is fortuitous, but alternatively that it may indicate that globular proteins and (weakly) charged hyperbranched AGPs carry some common volumetric behavior, at least similar proportionality between volume and adiabatic compressibility parameters. If this assumption is correct, one could expect to treat in deeper details AGP volumetric data, as was previously done for globular proteins by Gekko and Noguchi [60], Gekko and Hasegawa [32], Kharakoz and Sarvazian [36], but especially as reported by Chalikian and collaborators in a highly comprehensive series of articles [29,70,89,90].

4.1. Microscopic Description of AGP Volumetric Experimental Data

The estimation of molar volumes (V_M, V_T, V_l, V_h°) and molar adiabatic compressibilities (K_M, K_{sh}°, K_r) and hydration number (n_h) parameters was done on HIC fractions from A. *senegal* gum, i.e., HIC-F1, HIC-F2, and HIC-F3. Despite the tedious fractionation, it was important to remember that the HIC-fractions were more or less polydisperse (M_w/M_n: 1.3–1.9) and that the estimated volumetric parameters have to be considered as "average" for macromolecules with similar polar properties, but differing by their molar masses, size, shape, and charge density [15]. We found by HPSEC-MALS, with a M_w of 7.5×10^5 g·mol^{-1} as a subjective limit between low and high M_w macromolecules, that HIC-F1, HIC-F2, and HIC-F3 were composed by about 7%, 88%, and 67% of high M_w AGP. Keeping this limitation in mind, we first detailed the approach for HIC-F1 that presented the advantages to be the main specie in A. *senegal* gums ($\approx$80–85%), which then largely determines its physicochemical properties, to contain very low amount of proteins (0.5%), which were essentially neglected and a high amount of low M_w AGP (93%).

4.2. Partial Molar Volumes of AGPs

Knowing that the experimental V_s° was 1.95×10^5 cm^3·mol^{-1} (Table 5) and that the partial molar volume of bulk water at 25 °C V_o° was 18 cm^3·mol^{-1}, for describing volumetric properties of HIC-F1 we needed to estimate V_M, V_T, V_l and V_h° (Equations (8)–(10)). We first tried to estimate the intrinsic partial molar volume $V_M = (V_{vdW} + V_{void})$. For a significant number of globular proteins, V_M represented about 80–95% of the experimental V_s° [29,91]. Taking an average value of 90%, the average V_M was 176,296 cm^3·mol^{-1} (Table 5). We then calculated the van der Waals volume V_{vdW} by an additivity scheme that was based on the Bondi approach [64,92–94]. We took into consideration the sugar composition, the presence of minerals, and the contribution of covalent bonds (the branching characteristics of neutral sugars can be found in Supplementary Table S2). We obtained a final estimate for V_{vdW} of 143530 cm^3·mol^{-1}. We then calculated the partial molar volume of voids $V_{void} = (V_M - V_{vdW})$ as 32,766 cm^3·mol^{-1}. The packing density of the molecule ($\rho_M = V_{vdW}/V_M$), as previously indicated, for HIC-F1 was 0.818 (Table 5). This is close to the maximum value for closely packed spheres ($\approx$0.74) and the packing densities of organic crystals [41,59].

The packing density of HIC-F1 is close to the 0.87, value reported for nucleic acids [41], and to that of globular proteins that is in the 0.72–0.78 range [29,38]. HIC-F1 is then tightly packed with voids ($\approx$20% in average), which is an intrinsic property of hyperbranched polymers [95–98]. This view is consistent with the structure of HIC-F1, which is a thin ellipsoidal object with a dense outer shell and a highly dense porous central network, as indicated by the local fractal dimension of about 2.6 [17].

The partial molar thermal volume V_T can be approximated from the product of the total solvent accessible surface area (SASA, Å^2) and the thickness of the thermal volume (Å) [29,67]. The SASA parameter for HIC-F1 was first estimated using the average solvent accessible surface areas of atoms of carbon and oxygen from various linear and weakly branched polysaccharides [99,100]. The used values for C, O and O- were 10, 15.2 and 30.2 Å^2, respectively. We then obtained a total SASA estimate of about 84,000 Å^2. To check if this value is of an acceptable magnitude, we first considered as a rough approach the surface area of a homogeneous oblate ellipsoid with the dimensions proposed for HIC-F1 with semi-axis (Å) 96 × 96 × 14 [17]. We found a surface area of $\approx$62,000 Å^2. Since the surface of HIC-F1

is highly rough, an accessible surface area larger than 62,000 Å^2 was not unreasonable. It may be of interest to note that, using the M$_w$ of HIC-F1 and the power-law relationships SASA $\approx$ 5.3M$_w^{0.76}$, found for oligomeric proteins with M$_w$ up to 2×10^5 g·mol^{-1} [101,102], the SASA was 86,000 Å^2. In order to calculate V_T, we needed to estimate the thickness (Δ) of the thermal volume. Values that were between 0.5 and 1 Å have been calculated on small solutes and proteins [29,63,67,68]. The parameter Δ has been shown to depend on the solute size, and values of around 1 have been calculated for large solute [90]. We then took a Δ value of 1 Å. Multiplying the SASA estimation by 1 produced a thermal volume V_T of 84,000 Å^3 or 50,440 cm^3·mol^{-1} (Table 5). If a Δ value of 0.65 had been taken, as calculated for globular proteins by Bano and Marek (2005) [67], a value of 54,600 Å^3 or 33,000 cm^3·mol^{-1} should have been obtained. This should not fundamentally change the interpretation of our data, but obviously should impact the value of V_l, then of the hydration term (decrease).

Table 5. Volumetric parameters and hydration of HIC fractions (HIC-F1, HIC-F2, and HIC-F3) obtained from A. *senegal* gum by Hydrophobic Interaction chromatography (HIC). All of the measurements were done at 25 °C using pH 5 acetate buffer 10 mM.

Volumetric Properties	HIC-F1	HIC-F2	HIC-F3
Partial molar volumes and related parameters			
$V_s°$ Experimental partial molar volume (cm^3·mol^{-1})	195,715	878,462	1,038,047
V_M Intrinsic partial molar volume (cm^3·mol^{-1})	176,296	790,616	934,243
V_{vdw} vdW partial molar volume (cm^3·mol^{-1})	143,530	566,467	548,311
V_{void} void partial molar volume (cm^3·mol^{-1})	32,766	224,149	385,932
V_T thermal partial molar volume (cm^3·mol^{-1})	50,440	191,573	192,283
V_l interaction partial molar volume (cm^3·mol^{-1})	$-30,852$	$-103,727$	$-90,771$
V_{sh} Partial molar volume hydration water (cm^3·mol^{-1})	16.298	16.320	16.333
Decrease of partial molar volume of hydration water (%)	9.5	9.3	9.3
Packing density (V_{vdw}/V_M)	0.81	0.72	0.60
Void volume (%)	18.6	28.4	40.2
Hydration number n_h (mole H$_2$O/mole AGP)	18,128	61,748	54,444
Hydration number n_h (g$_{H2O}$/g$_{AGP}$)	0.85	0.68	0.54
Hydration number n_h (molecule H$_2$O/per residue)	9.0	6.8	5.1
Hydration number n_h per polysaccharide moiety (g$_{H2O}$/g AGP) [a]	0.88	0.72	0.62
Hydration number n_h per sugar residue of the Polysaccharide moiety (g$_{H2O}$/g$_{sugar\ residue}$)	8.5	6.6	5.8
Hydration number n_h per protein moiety (g$_{H2O}$/g$_{AGP}$) [a]	0.44	0.36	0.31
Hydration number n_h per amino acid residue of the Protein moiety (g$_{H2O}$/g$_{amino\ acid\ residue}$)	3.9	3.6	3.4
Partial molar adiabatic compressibility and related parameters			
K_M (cm^3·mol^{-1}·Pa^{-1}) Intrinsic molar adiabatic compressibility	1.88×10^{-5}	1.00×10^{-4}	1.49×10^{-4}
β_M (Pa^{-1}) Intrinsic coefficient of adiabatic compressibility	1.06×10^{-10}	1.27×10^{-10}	1.60×10^{-10}
Partial molar compressibility hydration water (cm^3·mol^{-1}·Pa^{-1})	5.20×10^{-9}	4.60×10^{-9}	5.30×10^{-9}
Partial specific compressibility hydration water (Pa^{-1})	2.91×10^{-10}	2.54×10^{-10}	2.95×10^{-10}
Decrease of partial molar adiabatic compressibility of Hydration water (%)	37	45	36

[a] estimated values considering that polysaccharides bound twice water than proteins.

Knowing $V_s°$, V_M and taking 84,000 Å^3 for V_T, we obtained for HIC-F1 an interaction volume V_l of about $-31,000$ cm^3·mol^{-1} (Table 5). We noted that V_l was close in absolute value to that of void volume V_{void}, as remarked previously for globular proteins [32]. V_l can be also estimated from the contribution of pentose and hexose type sugars. Thus, it was found that, on average, a monosaccharide in dilute solution, such as arabinose or galactose, contributed at 25 °C to around -28 cm^3·mol^{-1} to V_l and that a hydroxyl group OH contributed to -5 cm^3·mol^{-1} [103]. We do not know the contribution to V_l of charged groups, but, based on the double solvent-accessible surface area of charged oxygen atoms as compared to uncharged one, we supposed this contribution as the double than that of polar groups, i.e., -10 cm^3·mol^{-1}. From the sugar and amino acid composition, and the branching characteristics of HIC-F1, we estimated that the number of interacting polar and charged sites was in average around 2.8 per sugar residue. Then, an averaged polar or charged sugar residue effectively contributed to -15 cm^3·mol^{-1} to V_l. Multiplying this value by the number of sugar residues gives a V_l value of around ~-30000 cm^3·mol^{-1}, close to the estimated one.

Using the different volumes, it was possible to find the hydration number of HIC-F1 in dilute conditions through the equation: $V_l = n_h (V_h° - V_o°)$. We needed, however, to know the water volume contraction that was induced by the solute-water interaction, then the partial molar volume of interacting water $V_h°$. Interactions between chemical groups and water induce generally a water

volume contraction of about 5–10% for polar groups and 10–15% for charged groups [70]. A 10% increase in the density of hydration shell is commonly observed for biopolymers [41,104]. Taking an average value of 7.5% for polar groups and 12.5% for charged groups, $(V_h^\circ - V_o^\circ)$ was -1.7 cm$^3\cdot$mol^{-1} (9.3–9.5% water volume contraction). Then, n_h was in average 18,130 H$_2$O molecules per HIC-F1 molecule or 0.85 g H$_2$O$\cdot$g^{-1} AGP (Table 5).

The same analysis was done for the two other fractions HIC-F2 and HIC-F3. For these AGP, the amount of proteins cannot be longer neglected. However, in order to calculate the volumetric contribution of the protein part, we needed the protein M$_w$. When considering the percentages in proteins and the global M$_w$ (Tables 1 and 2), assuming a single averaged polypeptide, we get protein M$_w$ values for HIC-F2 and HIC-F3 of around 95,000 g$\cdot$mol^{-1} and 230,000 g$\cdot$mol^{-1}, respectively. Values comprised between 30,000 and 250,000 g$\cdot$mol^{-1} were proposed for the protein part of HIC-F2 [15,16,105] and a value of around 500,000 g$\cdot$mol^{-1} was proposed for HIC-F3 [15]. High M$_w$ values for the AGP protein cores probably indicated the presence of supramolecular structures, with many polypeptide chains in different glycoprotein modules [16,19]. Nevertheless, with these M$_w$ values, we estimated the global protein contribution to V_s°, V_M, and V_T using the approximate equations proposed for globular proteins [29]. Final calculations for HIC-F2 and HIC-F3 are indicated in Table 5. We first noted that the V_l/V_{void} ratio, in absolute value, was smaller than unity, which was a clear difference with HIC-F1. This was mainly due to the increase of the void volume with values for HIC-F2 and HIC-F3 of 28.4% and 40.2%, respectively (Table 5). This result can be connected to the above mentioned decrease of AGP density from HIC-F1 to HIC-F3 (Table 2), but also to previous microscopic experiments that showed a more open structure for HIC-F2, and especially HIC-F3, as noted in the introduction. The increase of V_{void} could be due both to the increase in the relative protein concentration (additive effect) and to more heterogeneous chain packing of massive sugar blocks and constrained proteins. Increasing the M$_w$ of hyperbranched polymers have been shown to promote an increase of the volume of voids [96–98,106]. In parallel, n_h decreased from HIC-F1 to HIC-F3 (as supposed from Figure 2), with values around 0.85, 0.68, and 0.54 g H$_2$O$\cdot$g^{-1} AGP, respectively, in agreement with the charged, polar, and nonpolar characteristics of the three fractions.

4.3. Partial Molar Adiabatic Compressibility of AGPs

Having estimated the partial molar volumes and hydration numbers, we turn now to the determination of adiabatic compressibility, then to the flexibility of macromolecules. We used the modified version of the Equation (10):

$$k_s^\circ = k_M + n_h \left(K_{sh}^\circ - K_{so}^\circ \right)/M_w + k_r \tag{12}$$

with the partial specific adiabatic compressibility k_s° (cm$^3\cdot$g$^{-1}\cdot$Pa^{-1}) equal to $k_s^\circ = K_s^\circ/M_w$, the intrinsic partial specific adiabatic compressibility $k_M = K_M/M_w$, and the relaxation term $k_r = K_r/M_w$. The parameter K_r is of a few percent for globular proteins and almost zero for unfolded polypeptides and nucleic acids that are more hydrated than globular proteins, then less flexible [35,37,41,107]. It was then neglected in the present analysis. We first considered HIC-F1 in some details, and then HIC-F2 and HIC-F3.

The parameter k_M was estimated based on the partial molar adiabatic compressibility of hydrating water K_{sh}° predicted for charged and polar groups [70], and on the peculiar hydration properties of hyperbranched polymers. K_{sh}° of water solvating charged groups is smaller than that of bulk water (20–60% decrease) and K_{sh}° of polar groups is between 80 and 110% of the bulk water value, depending on the chemical nature of other neighboring chemical groups in proximity. In addition, the compressibility of water in the hydration shell of the molecule is somewhat larger near apolar atoms [31,39]. For globular proteins, all of these contributions resulted in a global $\approx$20–35% decrease of K_{sh}° [29,36,37,39,108]. This value can further decrease down to 50–60% for highly hydrophilic proteins or highly pressurized globular proteins, indicating that stronger solute-water interactions

induced stronger perturbation of solvent adiabatic compressibility [30,108,109]. Stronger perturbation of hydrating water was also determined for highly branched polysaccharides or oligosaccharides as compared to linear ones or dendrimers, which can be due to strong water confinement within the hyperbranched architecture [110]. This can be probably related to the increased hydration of polar groups in close proximity to other polar groups [35,37,63,64]. Also, it is of interest to note that the surface roughness of biopolymers can significantly impact, through the existence of grooves and the strength of solute-water hydration [111]. Based on these different arguments, we took for K_{sh}° average values of 3.30×10^{-9} cm$^3 \cdot$mol$^{-1} \cdot$Pa^{-1} for charged groups60% decrease) and 2.48×10^{-9} cm$^3 \cdot$mol$^{-1} \cdot$Pa^{-1} for polar groups (30% decrease). We then obtained for HIC-F1 an average K_{sh}° value of 5.2×10^{-11} cm$^3 \cdot$mol$^{-1} \cdot$Pa^{-1} or 29×10^{-11} Pa^{-1}, corresponding to a 37% decrease as compared to bulk water (Table 5). Please note that this value is larger than the 18×10^{-11} Pa^{-1} arbitrary value that is usually used for characterizing the adiabatic compressibility of strongly hydrogen-bonded hydrating water of polysaccharides [45,47,50,51,54], but still of the same magnitude.

Using the assumed K_{sh}°, we found for HIC-F1 an intrinsic partial specific adiabatic compressibility k_M of 5.4×10^{-11} cm$^3 \cdot$g$^{-1} \cdot$Pa^{-1}, then a coefficient of adiabatic compressibility β_M of 10.6×10^{-11} Pa^{-1}, close to the 12–13×10^{-11} Pa^{-1} value found for ice [40,48,112–114]. This value is in the 3–10×10^{-11} Pa^{-1} range estimated for dextrans, carageenans, and starch polysaccharides based on volumetric measurements [44–46,52], and confirmed the intrinsic rigid nature of highly glycosylated AGPs. For globular proteins, ultrasonic measurements [29,31,36,115,116], and other experimental approaches or molecular dynamic simulations [28,108,117–121] have provided β_M values extrapolated at ambient pressure in the range 10–25×10^{-11} Pa^{-1}. Such value is considered as to be the most reliable value for globular proteins [38,40]. Since $\beta_M = \frac{B_M}{\rho_M}$, (Equation (13)), the coefficient of proportionality B_M for HIC-F1 was 8.7×10^{-11} Pa^{-1}, which was notably smaller than the 18.3×10^{-11} Pa^{-1} that was determined for globular proteins [29]. Consequently, the interior of HIC-F1 was less easily deformable than the interior of globular proteins, and then contributed to a less extent to the adiabatic compressibility. This can be in part related to the higher rigidity of sugar chains as compared to that of amino acid ones. It is known for long time that grafting glycan chains onto a protein resulted in a decrease of its flexibility [122]. Assuming that the B_M parameter was constant, we calculated the coefficients of adiabatic compressibility β_M for HIC-F2 and HIC-F3. We found, respectively, 12.7×10^{-11} Pa^{-1} and 16×10^{-11} Pa^{-1} for HIC-F2 and HIC-F3. Although all of the AGPs were intrinsically rigid, the flexibility was increasingly larger for species containing more proteins, in relation to the increase in volume fluctuations. Armed with the β_M values, we calculated the adiabatic compressibility of hydrating water, and we found that HIC-F2 and HIC-F3 hydration induced a decrease of K_{sh}° by 45% and 36%, respectively (Table 5). These results suggested that the strength of solute-water molecule interactions and the quality of hydration was not significantly different for the AGPs that were extracted from Acacia gum. This may be connected to the observation that, within each class of neutral monosaccharides (pentoses, hexoses), the contraction of water caused by each polar group is more or less the same [103]. In parallel, this suggested that the hydration ability of AGPs is mainly determined by the relative amount of charged, polar and nonpolar residues (the quantity of hydration) and the interior architecture of macromolecules.

4.4. Additional Comments on the Hydration Properties of AGPs

The question of the hydration of AGPs has not been considered in details in the past, probably because it seemed obvious that Acacia gums are by nature highly hydrophilic [4]. Indeed, the affinity of AGPs for water provides an extremely favorable environment for binding water, which is mainly due to the carbohydrate component of AGPs and in part to their highly branched characteristic [123]. For instance, intramolecular (and intermolecular) voids could be occupied by water in a variety of metastable states, thus preventing the formation of the ideal ice structure [123]. In addition, hyperbranched macromolecules may induce the formation of a well-ordered network of interacting

water molecules through the crowded environment between closely packed chains, as shown for phytoglycogen [110,124,125].

In the present study, we estimated hydration numbers of 0.85, 0.68, and 0.54 g $H_2O \cdot g^{-1}$ AGP for, respectively, HIC-F1, HIC-F2, and HIC-F3 (Table 5). We remember that the "hydration number (n_h)" refers to water molecules involved in the hydration shell, and then with significant perturbation of its physicochemical properties. These values are in the range of the 0.6–1.2 g $H_2O \cdot g^{-1}$ values of interacting "bound" water experimentally measured on Acacia *senegal* gum by water adsorption experiments or DSC [4,123,126], validating *a posteriori* the approximations we used for calculations. More specifically, values around 0.6–0.7 g $H_2O \cdot g^{-1}$ were found for raw A. *senegal* gum and values around 0.9–1.2 g $H_2O \cdot g^{-1}$ were found for calcium or sodium salts of the gum, showing the role of minerals on molecule hydration. This range is common for polysaccharides and can be compared to the usual values found for globular proteins (0.3–0.5 g $H_2O \cdot g^{-1}$). Then, when considering that polysaccharides were bound in general twice water than proteins, the peptide or protein part of HIC-F1, HIC-F2 and HIC-F3 contained approximatively 0.44, 0.36 and 0.31 g $H_2O \cdot g^{-1}$ protein (Table 5), respectively, which is coherent with the content in polar and nonpolar amino acids and in line with reported values for proteins. On the other hand, n_h of the polysaccharide moieties was estimated as 0.88, 0.72, and 0.62 g $H_2O \cdot g^{-1}$ AGP, for, respectively, HIC-F1, HIC-F2, and HIC-F3 (Table 5). This corresponded to n_h per sugar residue of, in average, 8.5, 6.6, and 5.8 g $H_2O \cdot g^{-1}$. Now, taking into account the 2.8 estimated averaged number of interacting polar and charged sites per sugar residue, n_h per interacting sites were in theory around 3.1, 2.4, and 2.1 for, respectively, HIC-F1, HIC-F2, and HIC-F3. These values can be compared to the 2.6–2.7 g H_2O per OH hydration number determined at 25 °C for arabinose and galactose, the two predominant sugars in Acacia gums [70], and more generally to the ~3 values that are usually found for monosaccharides and disaccharides in solution [124,127,128]. This result would indicate that the hydration shell of sugars that is involved in the hyperbranched structure of AGPs is not fundamentally different from that of isolated sugars. This is in clear contrast with (neutron scattering) results obtained on hyperbranched phytoglycogen, which revealed a n_h per polar sites of around 7, which was probably due to the crowded environment between the closely packed chains within the phytoglycogen particle and the existence of a well-ordered network of water molecules [110,124]. Thus, phytoglycogen can adsorb up to 2.6 g $H_2O \cdot g^{-1}$ polysaccharide [124].

Interestingly, like phytoglycogen, hyperbranched AGPs from Acacia gums may adsorb a maximum amount of 3–4 g $H_2O \cdot g^{-1}$ AGP, as determined from DSC experiments. This also indicated the formation of a three-dimensional network of AGP and water builds up as a structured entity [123]. We are then faced to an apparent contradiction, since sugars in AGPs displayed the same behavior than single sugars in solution, but a network of interacting water molecules seems to be created. One possible reason is that our estimate was based on the non-covalently bound polar and charged groups, without considering the likely existence of intramolecular hydrogen bonding between some of chemical groups. Strongly bound water is tightly associated with carbohydrate chains, which could form intramolecular hydrogen bonds within the highly cross-linked gum structure [123]. The presence of volume fluctuations in AGPs also suggests the existence of intramolecular hydrogen bonding. The question remains pending; however, higher n_h per interacting sites does not seem unreasonable for AGPs. Another possibility is that physicochemical properties of water hydrating Acacia gum, but not involved in hydration shell, is insufficiently perturbed to be probed using ultrasound measurements. This point also deserves more investigation, using other complementary methods, such as DSC, neutron scattering, or dielectric spectroscopy.

5. Concluding Remarks

This paper reports the first volumetric characterization of hyperbranched arabinogalactan (AGP) from Acacia gum. These properties are to a great extent determined by hydration and flexibility of macromolecules, two molecular characteristics that can be probed using combined sound and density

measurements and calculations of volumetric parameters, i.e., partial specific volume v_s° ($cm^3 \cdot g^{-1}$), and, for instance, coefficient of partial specific adiabatic compressibility β_s° (Pa^{-1}). We characterized both A. *senegal* and *seyal* gums and the three fractions that were obtained from the former by hydrophobic interaction chromatography (HIC). Fractions were named HIC-F1, HIC-F2, and HIC-F3, according to their order of elution, and then in the order of increased hydrophobicity.

For both total gums and HIC fractions, the adiabatic compressibility was negative, indicating that the hydration contribution was more important than the intrinsic molecular contribution. Changing the solvent quality did not markedly change the volumetric parameters of A. *senegal*, in line with the weak polyelectrolyte behavior of AGPs, excepted at high ionic strength where an increase of the v_s° parameter, then a decrease of hydration, was observed. In addition, the adiabatic compressibility (K_s°) of A. *senegal* was less negative than that of A. *seyal*, which is probably due to the larger arabinose content of the latter. Regarding HIC fractions, v_s° and K_s° were strongly dependent on their protein content, which in turn, largely determine their hydrophobicity. A larger protein content, like for HIC-F2 and HIC-F3, means a higher number of nonpolar amino acids and concomitantly a smaller number of polar and charged sugars, then a reduced hydration. Minerals contribute to this tendency through charge shielding. Thus, v_s° was larger and β_s° was less negative for the less polar HIC-F3. Plotting v_s° vs. β_s° with our AGP data and literature data obtained on globular proteins, polysaccharides and nucleic acids produced a curve that could be considered as a polarity-flexibility qualitative scale. In this curve, volumetric parameters of AGPs were intermediate between those of highly charged rigid polysaccharides and less polar more flexible globular proteins, highlighting the semi-rigid features of these hybrid protein-polysaccharide complexes. Due to this hybrid configuration, volumetric properties are better balanced for AGPs than for polysaccharides and proteins, which must play an important role in the ability of these biopolymers to rapidly adapt to various polarity environments and to interact with both polar and nonpolar molecules.

Based on volumetric parameters, biochemical composition, and basic structural characteristics, we tentatively described macroscopic thermodynamic properties of HIC fractions through microscopic molecular characteristics. We obtained molecular parameters that were not previously described for AGP, such as, for instance, the packing density, then the percentage of interior voids, and the intrinsic adiabatic compressibility, and then the macromolecular flexibility. The volume of voids increased with the AGP molar mass and hydrophobicity from about 20% for HIC-F1 to 40% for HIC-F3. The high value obtained for the latter is probably due both to the larger amount of protein, the effect of this larger amount of protein in the global AGP architecture and the formation of AGP assembly through mainly protein-protein interactions. In parallel, the intrinsic AGP rigidity decreased from HIC-F1 to HIC-F3, which is in line with an increase in molecular volume fluctuations. The hydration number of fractions was estimated and reasonable values in the range 0.5–0.9 $H_2O \cdot g^{-1}$ AGP were found, with obviously the larger values being found for the more polar fraction, i.e., HIC-F1. The amount of interacting water clearly depended on the chemical composition of fractions, but apparently not on the strength of water-AGP interaction. Due to the calculation estimations, this point needs to be experimentally confirmed by alternative methods. Averaged n_h of sugar residues constituting AGP did not appear to be significantly different from that of single monosaccharide in solution, in the case where all free possible interacting sites are considered. However, the existence of intramolecular hydrogen bonding between sugar chains in close proximity that contribute to volume fluctuations, are rather in favor of larger effective n_h per sugar residue. This suggests the presence of a network of water molecules, which a part may display similar physicochemical properties than bulk water.

In the aggregate, despite some rough approximations, our results demonstrated that protein-rich high molar mass HIC-F3 was the more flexible and the less hydrated AGP in A. *senegal* gum, while protein-poor low molar mass HIC-F1 was the less flexible and the more hydrated AGP, the HIC-F2 fraction exhibiting an intermediate behavior. These results can be connected to the known physicochemical properties of Acacia gums, especially their solubility behavior and their interfacial properties. In particular, while Acacia gums solubilize easily in water, through the major

contribution of the polar HIC-F1, it is known that HIC-F3 is a molecule where the solubility is strongly sensitive to solvent polarity, but also to the minimum water concentration reached upon fraction dehydration, either by freeze-drying or spray-drying. Regarding interfacial properties, the higher surface activity of HIC-F3 among the three fractions [129] can be related both to the larger percentage of volume fluctuations and to the lower macromolecular hydration ability. In terms of futures prospects, the same analyses will be made on highly purified HIC-F2 and HIC-F3 fractions in order to better take into account the inherent AGP polydispersity. Also, the question of the effect of AGP self-assembly, a property that is shared by all AGPs, on volumetric properties of gums needs to be considered.

Author Contributions: Verónica Mejia Tamayo contributed by designing, performing the experiments, analyzing data and writing the paper. Michaël Nigen contributed by performing experiments, analyzing data and writing the paper. Rafael Apolinar Valiente contributed with the purification of the Acacia gum fractions. Thierry Doco, Pascale Williams and Denis Renard contributed by writing the paper. Christian Sanchez contributed with analyzing data and writing the paper.

Conflicts of Interest: The authors declare no conflict of interest.

References

1. Williams, P.A.; Philips, G.O. Gum arabic. In *Handbook of Hydrocolloids*; CRC Press: Boca Raton, MA, USA, 2000; pp. 155–168.
2. Nussinovitch, A. *Plant Gum Exudates of the World: Sources, Distribution, Properties and Aplication*; CRC Press: Boca Raton, MA, USA, 2010.
3. Verbeken, D.; Dierckx, S.; Dewettinck, K. Exudate gums: Occurence, production, and applications. *Appl. Microbiol. Biot.* **2003**, *63*, 10–21. [CrossRef] [PubMed]
4. Sanchez, C.; Nigen, M.; Mejia Tamayo, V.; Doco, T.; Williams, P.; Amine, C.; Renard, D. Acacia gum: History of the future. *Food Hydrocoll.* **2017**. [CrossRef]
5. Akiyama, Y.; Eda, S.; Kato, K. Gum arabic is a kind of arabinogalactan protein. *Agric. Biol. Chem.* **1984**, *48*, 235–237.
6. Tan, L.; Showalter, A.M.; Egelund, J.; Hernandez-Sanchez, A.; Doblin, M.S.; Bacic, A. Arabinogalactan-proteins and the research challenges for these enigmatic plant cell surface proteoglycans. *Fronti. Plant Sci.* **2012**, *3*, 1–10. [CrossRef] [PubMed]
7. Lamport, D.T.A.; Várnai, P. Periplasmic arabinogalactan glycoproteins act as a calcium capacitor that regulates plant growth and development. *New Phytol.* **2013**, *197*, 58–64. [CrossRef] [PubMed]
8. Liu, C.G.; Mehdy, M.C. A nonclassical arabinogalactan protein gene highly expressed in vascular tissues agp31, is transcrptionally repressed by methyl jasmonic acid in arabidopsis. *Plant Physiol.* **2007**, *145*, 863–874. [CrossRef] [PubMed]
9. Ellis, M.; Egelund, J.; Schultz, C.J.; Bacic, A. Arabinogalactan-proteins: Key regulators at the cell surface? *Plant Physiol.* **2010**, *153*, 403–419. [CrossRef] [PubMed]
10. Showalter, A.M. Arabinogalactan-proteins: Structure, expression and function. *Cell. Mol. Life Sci.* **2001**, *58*, 1399–1417. [CrossRef] [PubMed]
11. Qu, Y.M.; Egelund, J.; Gilson, P.R.; Houghton, F.; Gleeson, P.A.; Schultz, C.J.; Bacic, A. Identification of a novel group of putative arabidopsis thaliana beta-(1,3)-galactosyltransferases. *Plant Mol. Biol.* **2008**, *68*, 43–59. [CrossRef] [PubMed]
12. Anderson, D.M.W.; Stoddart, J.F. Studies on uronic acid materials. Part xv. The use of molecular-sieve chromatography on *acacia senegal* gum (gum arabic). *Carbohydr. Res.* **1966**, *2*, 104–114. [CrossRef]
13. Randall, R.C.; Phillips, G.O.; Williams, P.A. Fractionation and characterization of gum from acacia *senegal*. *Food Hydrocoll.* **1989**, *3*, 65–75. [CrossRef]

14. Islam, A.M.; Phillips, G.O.; Sljivo, A.; Snowden, M.J.; Williams, P.A. A review of recent developments on the regulatory, structural and functional aspects of gum arabic. *Food Hydrocoll.* **1997**, *11*, 493–505. [CrossRef]

15. Renard, D.; Lavenant-Gourgeon, L.; Ralet, M.C.; Sanchez, C. Acacia senegal gum: Continuum of molecular species differing by their protein to sugar ratio; molecular weight; and charges. *Biomacromolecules* **2006**, 2637–2649. [CrossRef] [PubMed]

16. Mahendran, T.; Williams, P.; Phillips, G.; Al-Assaf, S.; Baldwin, T. New insights into the structural characteristics of the arabinogalactan-protein (agp) fraction of gum arabic. *J. Agric. Food Chem.* **2008**, *56*, 9269–9276. [CrossRef] [PubMed]

17. Sanchez, C.; Schmitt, C.; Kolodziejczyk, E.; Lapp, A.; Gaillard, C.; Renard, D. The acacia gum arabinogalactan fraction is a thin oblate ellipsoid: A new model based on small-angle neutron scattering and ab initio calculation. *Biophys. J.* **2008**, *94*, 629–639. [CrossRef] [PubMed]

18. Renard, D.; Garnier, C.; Lapp, A.; Schmitt, C.; Sanchez, C. Structure of arabinogalactan-protein from acacia gum: From porous ellipsoids to supramolecular architectures. *Carbohydr. Polym.* **2012**, *90*, 322–332. [CrossRef] [PubMed]

19. Renard, D.; Lavenant-Gourgeon, L.; Lapp, A.; Nigen, M.; Sanchez, C. Enzymatic hydrolysis studies of arabinogalactan-protein structure from acacia gum: The self-similarity hypothesis of assembly from a common building block. *Carbohydr. Polym.* **2014**, *112*, 648–661. [CrossRef] [PubMed]

20. Renard, D.; Lepvrier, E.; Garnier, C.; Roblin, P.; Nigen, M.; Sanchez, C. Structure of glycoproteins from acacia gum: An assembly of ring-like glycoproteins modules. *Carbohydr. Polym.* **2014**, *99*, 736–747. [CrossRef] [PubMed]

21. Lopez-Torrez, L.; Nigen, M.; Williams, P.; Doco, T.; Sanchez, C. Acacia *senegal* vs. Acacia *seyal* gums—part 1: Composition and structure of hyperbranched plant exudates. *Food Hydrocoll.* **2015**, *51*, 41–53. [CrossRef]

22. Renard, D.; Garnier, C.; Lapp, A.; Schmitt, C.; Sanchez, C. Corrigendum to "structure of arabinogalactan-protein from acacia gum: From porous ellipsoids to supramolecular architectures" [carbohydr. Polym. 90 (2012) 322–332]. *Carbohydr. Polym.* **2013**, *97*, 864–867. [CrossRef] [PubMed]

23. Ray, A.K.; Bird, P.B.; Iacobucci, G.A.; Clark, B.C. Functionality of gum arabic. Fractionation, characterization and evaluation of gum fractions in citrus oil emulsions and model beverages. *Food Hydrocoll.* **1995**, *9*, 123–131. [CrossRef]

24. Idris, O.H.M.; Williams, P.A.; Phillips, G.O. Characterisation of gum from acacia *senegal* trees of different age and location using multidetection gel permation chromatography. *Food Hydrocoll.* **1998**, 379–388. [CrossRef]

25. Dror, Y.; Cohen, Y.; Yerushalmi-Rozen, R. Structure of gum arabic in aqueous solution. *J. Polym. Sci. Pol. Phys.* **2006**, *44*, 3265–3271. [CrossRef]

26. Wang, Q.; Burchard, W.; Cui, S.W.; Huang, X.Q.; Philips, G.O. Solution properties of conventional gum arabic and a matured gum arabic (acacia (sen) super gum). *Biomacromolecules* **2008**, *9*, 1163–1169. [CrossRef] [PubMed]

27. Al-Assaf, S.; Sakata, M.; McKenna, C.; Aoki, H.; Phillips, G.O. Molecular associations in acacia gums. *Struct. Chem.* **2009**, *20*, 325–336. [CrossRef]

28. Kharakoz, D.P. Protein compressibility, dynamics, and pressure. *Biophys. J.* **2000**, *79*, 511–525. [CrossRef]

29. Chalikian, T.V.; Totrov, M.; Abagyan, R.; Breslauer, K.J. The hydration of globular proteins as derived from volume and compressibility measurements: Cross correlating thermodynamic and structural data. *J. Mol. Biol.* **1996**, *260*, 588–603. [CrossRef] [PubMed]

30. Scharnagl, R.M.; Friedrich, J. Local compressibilities of compressibilities: Comparison of optical experiments and simulations for horse heart cytochrome-c. *Biophys. J.* **2005**, *89*, 64–75. [CrossRef] [PubMed]

31. Gavish, B.; Gratton, E.; Hardy, C.J. Adiabatic compressibility of globular proteins. *Proc. Natl. Acad. Sci. USA* **1983**, *80*, 750–754. [CrossRef] [PubMed]

32. Gekko, K.; Hasegawa, Y. Compressibility-structure relationship of globular proteins. *Biochemistry* **1986**, *25*, 6563–6571. [CrossRef] [PubMed]

33. Durchschlag, H. Specific volumes of biological macromolecules and some other molecules of biological interest. In *Thermodynamic Data for Biochemistry and Biotechnology*; Hinz, H.-J., Ed.; Springer: Berlin, Germany, 1986; pp. 45–128.

34. Gekko, K. Hydration-structure-function relationships of polysaccharides and proteins. *Food Hydrocoll.* **1989**, *3*, 289–299. [CrossRef]

35. Sarvazyan, A.P. Ultrasonic velocimetry of biological compounds. *Annu. Rev. Biophys. Biophys. Chem.* **1991**, *20*, 321–342. [CrossRef] [PubMed]

36. Kharakoz, D.P.; Sarvazyan, A.P. Hydrational and intrinsic compressibilities of globular proteins. *Biopolymers* **1993**, *33*, 11–26. [CrossRef] [PubMed]

37. Chalikian, T.V.; Sarvazyan, A.P.; Breslauer, K.J. Hydration and partial compressibility of biological compounds. *Biophys. Chem.* **1994**, *51*, 89–109. [CrossRef]

38. Chalikian, T.V.; Filfil, R. How large are the volume changes accompanying protein transitions and binding? *Biophys. Chem.* **2003**, *104*, 489–499. [CrossRef]

39. Dadarlat, V.M.; Post, C.B. Decomposition of protein experimental compressibility into intrinsic and hydration shell contributions. *Biophys. J.* **2006**, *91*, 4544–4554. [CrossRef] [PubMed]

40. Gekko, K. Volume and compressibility of proteins. In *High Pressure Bioscience: Basic Concepts, Applications and Frontiers*; Akasaka, K., Matsuki, H., Eds.; Springer: Dordrecht, The Netherlands, 2015; pp. 75–108.

41. Buckin, V.A.; Kankiya, B.I.; Sarvazyan, A.P.; Uedaira, H. Acoustical investigation of poly(da)-poly(dt), poly[d(a-t)]-poly[d(at)], poly (a).Polyflj) and DNA hydration in dilute aqueous solutions. *Nucleic Acids Res.* **1989**, *17*, 4189–4203. [CrossRef] [PubMed]

42. Chalikian, T.V.; Sarvazyan, A.P.; Plum, S.G.E.; Breslauer, K.J. Influence of base composition, base sequence, and duplex structure on DNA hydration: Apparent molar volumes and apparent molar adiabatic compressibilities of synthetic and natural DNA duplexes at 25 °C. *Biochemistry* **1994**, *33*, 2394–2401. [CrossRef] [PubMed]

43. Chalikian, T.V.; McGregor, J.R.B. Nucleic acid hydration: A volumetric perspective. *Phys. Life Rev.* **2007**, *4*, 91–115. [CrossRef]

44. Myahara, Y.; Shio, H. The adiabatic compressibility of starch sols. *Nippon Kagaku Zasshi* **1952**, *73*, 1–2. [CrossRef]

45. Shiio, H.; Yoshihashi, H. Measurement of the amount of bound water by ultrasonic interferometer. Ii. Polyvinyl alcohol and its partially substituted acetates. *J. Phys. Chem.* **1956**, *60*, 1049–1051. [CrossRef]

46. Itoh, K. Adiabatic compressibility of polysaccharides. *Nippon Kagaku Zasshi* **1956**, *77*, 1594–1595. [CrossRef]

47. Nomura, H.; Miyahara, Y. Partial specific compressibility of polystyrene. *J. Appl. Polym. Sci.* **1964**, *8*, 1643–1649. [CrossRef]

48. Suzuki, Y.; Uedaira, H. Hydration of potassium hyaluronate. *Bull. Chem. Soc. Jpn.* **1970**, *43*, 1892–1894. [CrossRef]

49. Gekko, K.; Noguchi, H. Physicochemical studies of oligodextran. I. Molecular weight dependence of intrinsic viscosity, partial specific compressibility and hydrated water. *Biopolymers* **1971**, *10*, 1513–1524. [CrossRef] [PubMed]

50. Gekko, K.; Noguchi, H. Hydration behavior of ionic dextran derivatives. *Macromolecules* **1974**, *7*, 224–229. [CrossRef] [PubMed]

51. Kawaizumi, F.; Nishio, N.; Nomura, H.; Miyahara, Y. Calorimetric and compressibility study of aqueous solutions of dextran with special reference to hydration and structural change of water. *Polym. J.* **1981**, *13*, 209–213. [CrossRef]

52. Nomura, H.; Onoda, M.; Miyahara, Y. Preferential solvation of dextran in water—ethanol mixtures. *Polym. J.* **1982**, *14*, 249–253. [CrossRef]

53. Davies, A.; Gormally, J.; Wyn-Jones, E.; Wedlock, D.J.; Phillips, G.O. A study of factors influencing hydration of sodium hyaluronate from compressibility and high precision densimetric measurements. *Biochem. J.* **1983**, *213*, 363–369. [CrossRef] [PubMed]

54. Gekko, K.; Mugishima, H.; Koga, S. Compressibility, densimetric and calorimetric studies of hydration of carrageenans in the random form. *Int. J. Biol. Macromol.* **1985**, *7*, 57–63. [CrossRef]

55. Kupke, D.W. Density and volume change measurements. In *Physical Principles and Techniques of Protein Chemistry, Part C*; Leach, S.J., Ed.; Academic Press: Cambridge, MA, USA, 1973; pp. 3–75.

56. Hoiland, H. Partial molar volumes of biochemical model compounds in aqueous solution. In *Thermodynamic Data for Biochemistry and Biotechnology*; Hinz, H.-J., Ed.; Springer-Verlag: Berlin/Heidelberg, Germany, 1986; pp. 17–44.

57. Gekko, K.; Yamagami, K. Flexibility of food proteins as revealed by compressibility. *J. Agric. Food Chem.* **1991**, *39*, 57–62. [CrossRef]

58. Chalikian, T.V.; Sarvazyan, A.P.; Breslauer, K.J. Partial molar volumes, expansibilities, and compressibilities of.Alpha.,.Omega.-aminocarboxylic acids in aqueous solutions between 18 and 55 °C. *J. Phys. Chem.* **1993**, *97*, 13017–13026. [CrossRef]

59. Taulier, N.; Chalikian, T.V. Compressibility of protein transitions. *BBA-Protein Struct. Mol.* **2002**, *1595*, 48–70. [CrossRef]

60. Gekko, K.; Noguchi, H. Compressibility of globular proteins in water at 25 °C. *J. Phys. Chem.* **1979**, *83*, 2706–2714. [CrossRef]

61. Pierotti, R.A. A scaled particle theory of aqueous non aqueous solutions. *Chem. Rev.* **1976**, *76*, 717–726. [CrossRef]

62. Reiss, H. Scaled particle methodsin the statistical thermodynamics of fluids. *Adv. Chem. Phys.* **1965**, *9*, 1–84.

63. Kharakoz, D.P. Volumetric properties of proteins and their analogs in diluted water solutions. *Biophys. Chem.* **1989**, *34*, 115–125. [CrossRef]

64. Kharakoz, D.P. Partial volumes of molecules of arbitrary shape and the effect of hydrogen bonding with water. *J. Solut. Chem.* **1992**, *21*, 569–595. [CrossRef]

65. Pierotti, R.A. The solubility of gases in liquids. *J. Phys. Chem.* **1963**, *67*, 1840–1845. [CrossRef]

66. Kauzmann, W. Some factors in the interpretation of protein denaturation. *Adv. Protein Chem.* **1959**, *14*, 1–63. [PubMed]

67. Bánó, M.; Marek, J. How thick is the layer of thermal volume surrounding the protein? *Biophys. Chem.* **2006**, *120*, 44–54. [CrossRef] [PubMed]

68. Edward, J.T.; Farrell, P.G. Relation between van der waals and partial molal volumes of organic molecules in water. *Can. J. Chem.* **1975**, *53*, 2965–2970. [CrossRef]

69. Voloshin, V.P.; Medvedev, N.N.; Smolin, N.; Geiger, A.; Winter, R. Exploring volume, compressibility and hydration changes of folded proteins upon compression. *Phys. Chem. Chem. Phys.* **2015**, *17*, 8499–8508. [CrossRef] [PubMed]

70. Chalikian, T.V. Structural thermodynamics of hydration. *J. Phys. Chem. B* **2001**, *105*, 12566–12578. [CrossRef]

71. Kharakoz, D.P. Volumetric properties of proteins and their analogues in diluted water solutions. 2. Partial adiabatic compressibilities of amino acids at 15–70.Degree.C. *J. Phys. Chem.* **1991**, *95*, 5634–5642. [CrossRef]

72. Anderson, D.M.W.; Bridgeman, M.M.E.; Farquhar, J.G.K.; McNab, C.G.A. The chemical characterization of the test article used in toxicological studies of gum arabic (acacia *senegal* (l.) willd). *Int. Tree Crops J.* **1983**, *2*, 245–254. [CrossRef]

73. Flindt, C.; Alassaf, S.; Phillips, G.; Williams, P. Studies on acacia exudate gums. Part v. Structural features of acacia *seyal*. *Food Hydrocoll.* **2005**, *19*, 687–701. [CrossRef]

74. Hölter, D.; Burgath, A.; Frey, H. Degree of branching in hyperbranched polymers. *Acta Polym.* **1997**, *48*, 30–35. [CrossRef]

75. Gashua, I.B.; Williams, P.A.; Yadav, M.P.; Baldwin, T.C. Characterisation and molecular association of nigerian and sudanese acacia gum exudates. *Food Hydrocoll.* **2015**, *51*, 405–413. [CrossRef]

76. Osman, M.E.; Menzies, A.R.; Williams, P.A.; Phillips, G.O.; Baldwin, T.C. The molecular characterisation of the polysaccharide gum from acacia senegal. *Carbohydr. Res.* **1993**, *246*, 303–318. [CrossRef]

77. Chen, C.-G.; Pu, Z.-Y.; Moritz, R.L.; Simpson, R.J.; Bacic, A.; Clarke, A.E.; Mau, S.-L. Molecular cloning of a gene encoding an arabinogalactan-protein from pear (pyrus communis) cell suspension culture. *Proc. Natl. Aca. Sci. USA* **1994**, *91*, 10305–10309. [CrossRef]

78. Goodrum, L.J.; Patel, A.; Leykam, J.F.; Kieliszewski, M.J. Gum arabic glycoprotein contains glycomodules of both extensin and arabinogalactan-glycoproteins. *Phytochemistry* **2000**, *54*, 99–106. [CrossRef]

79. Al-Assaf, S.; Phillips, G.; Williams, P. Studies on acacia exudate gums: Part ii. Molecular weight comparison of the vulgares and gummiferae series of acacia gums. *Food Hydrocoll.* **2005**, *19*, 661–667. [CrossRef]

80. Sanchez, C.; Renard, D.; Robert, P.; Schmitt, C.; Lefebvre, J. Structure and rheological properties of acacia gum dispersions. *Food Hydrocoll.* **2002**, *16*, 257–267. [CrossRef]

81. Zhu, C.; Gao, Y.; Li, H.; Meng, S.; Li, L.; Francisco, J.S.; Cheng Zeng, X. Characterizing hydrophobicity of amino acid side chains in a protein environment via measuring contact angle of a water nonodroplet on planar peptide network. *PNAS* **2016**, *113*, 12946–12951. [CrossRef] [PubMed]

82. Shahidi, F.; Farrell, P.G.; Edward, J.T. Partial molar volumes of organic compounds in water. Iii. Carbohydrates. *J. Solut. Chem.* **1976**, *5*, 807–816. [CrossRef]

83. Banipal, P.K.; Banipal, T.S.; Lark, B.S.; Ahluwalia, J.C. Partial molar heat capacities and volumes of some mono-, di- and tri-saccharides in water at 298.15, 308.15 and 318.15 k. *J. Chem. Soc. Faraday Trans.* **1997**, *93*, 81–87. [CrossRef]

84. Perkins, S.J.; Miller, A.; Hardingham, T.E.; Muir, H. Physical properties of the hyaluronate binding region of proteoglycan from pig laryngeal cartilage: Densitometric and small-angle neutron scattering studies of carbohydrates and carbohydrate-protein macromolecules. *J. Mol. Biol.* **1981**, *150*, 69–95. [CrossRef]

85. Durchschlag, H. Determination of the partial specific volume of conjugated proteins. *Colloid Polym. Sci.* **1989**, *267*, 1139–1150. [CrossRef]

86. Tamura, Y.; Gekko, K.; Yoshioka, K.; Vonderviszt, F.; Namba, K. Adiabatic compressibility of flagellin and flagelar filament of *salmonella typhimurium*. *Biochim. Biophys. Acta* **1997**, *1335*, 120–126. [CrossRef]

87. Chalikian, T.V.; Völker, J.; Srinivasan, A.R.; Olson, W.; Breslauer, K.J. The hydration of nucleic acids duplexes as assessed by a combination of volumetric and structural techniques. *Biopolymers* **1999**, *50*, 459–471. [CrossRef]

88. Vandevelde, M.C.; Fenyo, J.C. Estimation of the charge density of arabic acid by potentiometry and dye binding. *Polym. Bull.* **1987**, *18*, 47–51. [CrossRef]

89. Chalikian, T.V. On the molecular origins of volumetric data. *J. Phys. Chem. B* **2008**, *112*, 911–917. [CrossRef] [PubMed]

90. Patel, N.; Dubins, D.N.; Pomes, R.; Chalikian, T.V. Size dependence of cavity volume: A molecular dynamics study. *Biophys. Chem.* **2012**, *161*, 46–49. [CrossRef] [PubMed]

91. Chen, C.R.; Makhatadze, G.I. Protein volume: Calculating molecular van der waals and void volume in proteins. *BMC Bioinf.* **2015**, *16*, 101–106. [CrossRef] [PubMed]

92. Bondi, A. Van der waals volumes and radii. *J. Phys. Chem.* **1964**, *68*, 441–451. [CrossRef]

93. Spillane, W.J.; Birch, G.G.; Drew, M.G.B.; Bartolo, I. Correlation of computed van der waals and molecular volumeswith apparent molar volumes (amw) for amino acid, carbohydrate and sulfamate tastant molecules. Relationship between corey-pauling-koltun volumes (vcpk) and computed volumes. *Chem. Soc. Perkin Trans.* **1992**, *2*, 497–523. [CrossRef]

94. Batsanov, S.S. Van der waals radii of elements. *Inorg. Mater.* **2001**, *37*, 871–885. [CrossRef]

95. Carl, W. A monte carlo study of model dendrimers. *J. Chem. Soc. Faraday Trans.* **1996**, *92*, 4151–4154. [CrossRef]

96. Maiti, P.K.; Cagin, T.; Lin, S.-T.; Williamm, A.G. Effect of solvent and ph on the structure of pamam dendrimers. *Macromolecules* **2005**, *38*, 979–991. [CrossRef]

97. Li, T.; Honk, K.; Porcar, L.; Verduzco, R.; Butler, P.D.; Smith, G.S.; Liu, Y.; Wei-Ren Chen, W.R. Assess the intramolecular cavity of a pamam dendrimer in aqueous solution by small-angle neutron scattering. *Macromolecules* **2008**, *41*, 8916–8920. [CrossRef]

98. Maiti, P.K. Pamam dendrimer: A ph controlled nanosponge. *Can. J. Chem.* **2017**, *95*, 991–998. [CrossRef]

99. Kaliannan, P.; Gromiha, M.M.; Elanthiraiyan, M. Solvent accesibility studies on polysaccharides. *Int. J. Biol. Macromol.* **2001**, *28*, 135–141. [CrossRef]

100. Kaliannan, P.; Gromiha, M.M.; Ramamurthi, K.; Elanthiraiyan, M. Solvent accesibility studies on glycosaminoglycans. *Biophys. Chem.* **1998**, *74*, 135–141. [CrossRef]

101. Miller, S.; Lesk, A.M.; Janin, J.; Chothia, C. The accesible surface area and stability of oligomeric proteins. *Nature* **1987**, *328*, 834–836. [CrossRef] [PubMed]

102. Janin, J.; Miller, S.; Chothia, C. Surface, subunit interfaces and interior of oligomeric proteins. *Mol. Biol.* **1988**, *204*, 155–164. [CrossRef]

103. Chalikian, T.V.; Breslauer, K.J. Thermodynamic analysis of biomolecules: A volumetric approach. *Curr. Opin. Struct. Biol.* **1998**, *8*, 657–664. [CrossRef]

104. Svergun, D.I.; Richard, S.; Koch, M.H.J.; Sayers, Z.; Kuprin, S.; Zaccai, G. Protein hydration in solution: Experimental observation by x-ray and neutron scattering. *PNAS* **1998**, *95*, 2267–2272. [CrossRef] [PubMed]

105. Qi, W.; Fong, C.; Lamport, T.A. Gum arabic glycoprotein is a twisted hairy rope. A new model based on o-galactosylhydroxyproline as the polysaccharide attachment site. *Plant Physiol.* **1991**, *96*, 848–855. [CrossRef] [PubMed]

106. Maiti, P.K.; Cagin, T.; Wang, G.; Goddard, W.A. Structure of pamam dendrimers: Generations 1 through 11. *Macromolecules* **2004**, *37*, 6236–6254. [CrossRef]

107. Sarvazyan, A.P.; Hemmes, P. Relaxational contributios to protein compressibility from ultasonic data. *Biopolymers* **1979**, *18*, 3015–3024. [CrossRef]

108. Marchi, M. Compressibility of cavities and biological water from voronoi volumes in hydrated proteins. *J. Phys. Chem. B* **2003**, *107*, 834–836. [CrossRef]

109. Smolin, N.; Winter, R. A molecular dynamics simulation of snase and its hydration shell at high temperature and high pressure. *Biochim. Biophys. Acta* **2006**, *1764*, 522–534. [CrossRef] [PubMed]

110. Grossutti, M.; Dutcher, J.R. Correlation between chain architecture and hydration water structure in polysaccharides. *Biomacromolecules* **2016**, *17*, 1198–1204. [CrossRef] [PubMed]

111. Kuhn, L.A.; Siani, M.A.; Pique, M.E.; Fisher, C.L.; Getzoff, E.D.; Tainer, J.A. The interdependence of protein surface topography and bound water molecules revealed by surface accessibility and fractal density measures. *J. Mol. Biol.* **1992**, *228*, 13–22. [CrossRef]

112. Smith, A.H.; Lawson, A.W. The velocity of sound in water as a function of temperature and pressur. *J. Chem. Phys.* **1954**, *22*, 351–359. [CrossRef]

113. Leadbetter, A.J. The thermodynamic and vibrational properties of h$_2$o ice and d$_2$o ice. *Proc. R. Soc. Lond.* **1965**, *287*, 403–425. [CrossRef]

114. Chen, Y.-C. *Review of Thermal Properties of Snow, Ice and Sea Ice*; Cold Regions Research and Engineering Laboratory: Hanover, NH, USA, 1981; pp. 1–35.

115. Jacobson, B. On the adiabatic compressibility of aqueous solutions. *Ark. Kemi* **1950**, *2*, 177–210.

116. Priev, A.; Almagor, A.; Yedgar, S.; Gavish, B. Glycerol decreases the volume and compressibility of protein interior. *Biochemistry* **1996**, *35*, 2061–2066. [CrossRef] [PubMed]

117. Edwards, C.; Palmer, S.B.; Helliwell, J.R.; Glover, D.; Harris, G.W.; Moss, D.S. Thermal motion in proteins estimated using laser-generated ultrasound and young's modulus measurements. *Acta Crystallogr.* **1990**, *A46*, 315–320. [CrossRef]

118. Morozov, V.N.; Morozova, T.Y. Elasticity of globular proteins. The relation between mechanics, thermodynamics and mobility. *J. Biomol. Struct. Dyn.* **1993**, *11*, 459–481. [CrossRef] [PubMed]

119. Paci, E.; Velikson, B. On the volume of macromolecules. *Biopolymers* **1996**, *41*, 785–797. [CrossRef]

120. Mori, K.; Seki, Y.; Yamada, Y.; Matsumoto, H.; Soda, K. Evaluation of intrinsic compressibility of proteins by molecular dynamics simulations. *J. Chem. Phys.* **2006**, *125*. [CrossRef] [PubMed]

121. Li, H.; Yamada, H.; Akasaka, K. Effect of pressure on individual hydrogen bonds in proteins: Basic pancreatic trypsin inhibitor. *Biochemistry* **1998**, *37*, 1167–1173. [CrossRef] [PubMed]

122. Wormald, M.R.; Petrescu, A.J.; Pao, Y.-L.; Glithero, A.; Elliot, T.; Dwek, R.A. Conformational studies of oligosaccharides and glycopeptides: Complementarity of nmr, x-ray crystallography, and molecular modelling. *Chem. Rev.* **2002**, *102*, 371–386. [CrossRef] [PubMed]

123. Phillips, G.O.; Takigami, S.; Takigami, M. Hydration characteristics of the gum exudate from *acacia senegal*. *Food Hydrocoll.* **1996**, *10*, 11–19. [CrossRef]

124. Nickels, J.D.; Atkinson, J.; Papp-Szabo, E.; Stanley, C.; Diallo, S.O.; Perticaroli, S.; Baylis, B.; Mahon, P.; Ehlers, G.; Katsaras, J.; et al. Structure and hydration of highly-branched, monodisperse phytoglycogen nanoparticles. *Biomacromolecules* **2016**, *17*, 735–743. [CrossRef] [PubMed]

125. Ramadugu, S.K.; Chung, Y.-H.; Xia, J.; Margulis, C.J. When sugars get wet. A comprehensive study of the behavior of water on the surface of oligosaccharides. *J. Phys. Chem. B* **2009**, *113*, 11003–11015. [CrossRef] [PubMed]

126. Hatakeyama, T.; Uetake, T.; Hatakeayama, H. Frezeeing bound water restrained by gum arabic. In *Gums and Stabilizers for the Food Industry*; RSC Publishing: Cambridge, UK, 2010; Volume 15, pp. 69–75.

127. Lupi, L.; Comez, L.; Paolantoni, M.; Perticaroli, S.; Sassi, P.; Morresi, A.; Ladanyi, B.M.; Fioretto, D. Hydration and aggregation in mono- and disaccharide aqueous solutions by gigahertz-to-terahertz light scattering and molecular dynamics simulations. *J. Phys. Chem. B* **2012**, *116*, 14760–14767. [CrossRef] [PubMed]

128. Perticaroli, S.; Nakanishi, M.; Pashkovski, E.; Sokolov, A.P. Dynamics of hydration water in sugars and peptides solutions. *J. Phys. Chem. B* **2013**, *117*, 7729–7736. [CrossRef] [PubMed]

129. Castellani, O.; Al-Assaf, S.; Axelos, M.; Phillips, G.O.; Anton, M. Hydrocolloids with emulsifying capacity. Part 2—Adsorption properties at the n-hexadecane–water interface. *Food Hydrocoll.* **2010**, *24*, 121–130. [CrossRef]